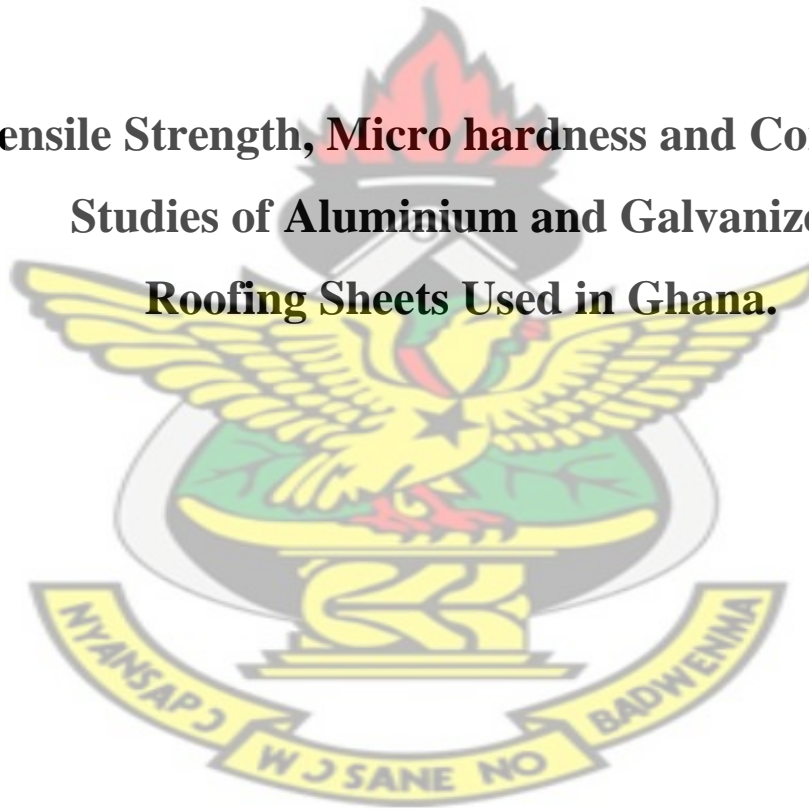**Kwame Nkrumah University of Science and Technology, Kumasi**

COLLEGE OF SCIENCE
DEPARTMENT OF PHYSICS

KNUST

Tensile Strength, Micro hardness and Corrosion Studies of Aluminium and Galvanized Roofing Sheets Used in Ghana.

BY

STEPHEN AGYEI   B.SC (HONS)

MARCH 2014

DECLARATION

I hereby declare that this thesis is my own work towards the MSc degree and to the best of my knowledge, it does not contain any materials previously published by another person nor materials which has been accepted by this university for any degree, except where due acknowledgement has been made in the text.

Stephen Agyei   …………………………………   ……………………

Student: Signature   Date

Dr. B. Kwakye-Awuah   …………………………………   ……………………

Supervisor   Signature   Date

Prof. S. K. Danuor   …………………………………   ……………………
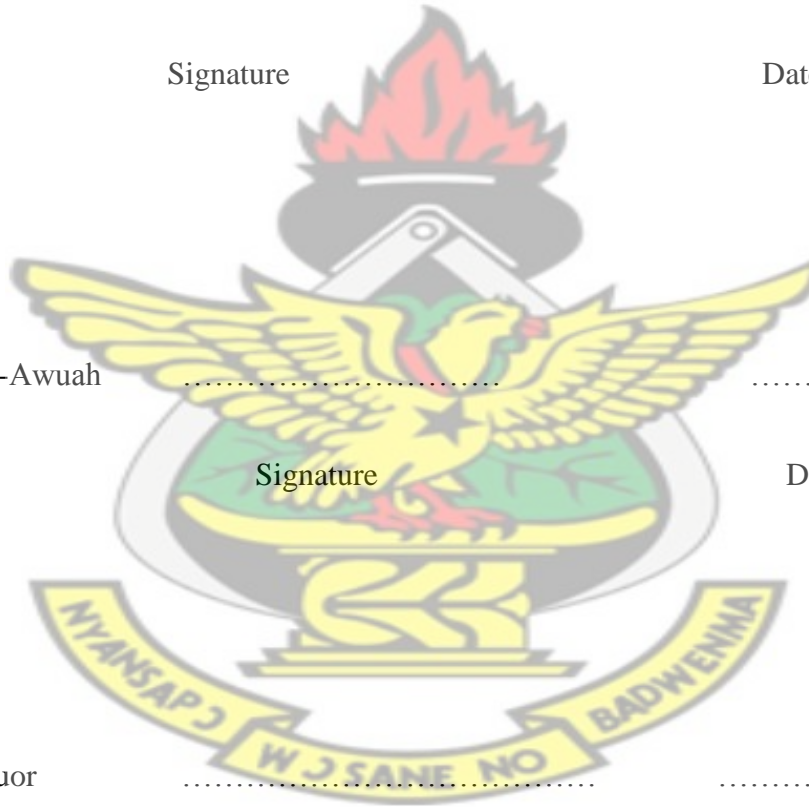
Head of Department   Signature   Date

DEDICATION

This thesis is dedicated to Parents, and daughter (Nana Afia agyei Amponsem).

ACKNOWLEDGEMENTS

ABSTRACT

The research objective was to study the tensile strength and micro hardness of aluminium and galvanized roofing sheets used in Ghana and the effect of corrosion on them. The roofing sheets were One star Galvanized Japan [G1*Jap], Galvanized Coated [GC]. Aluzinc three star galvanized [AlZn3*], One Star Galvanized Indi [G1*Ind] and Aluminium [Al]. The roofing sheets were then cut into dimensions of 5 cm x 5 cm for the micro hardness tests and 2 cm x 25 cm for the tensile tests. These samples for the tensile tests were machined at the mid portions to width of 1.6 cm. The corrosion samples were cut into 2 cm x 5 cm. The tensile tests were carried out using a Tinius Olsen Super 'L' hydraulic Universal Testing Machine. The computer interface with the machine returned values for the Modulus of Elasticity, Yield Strength, Ultimate Tensile Strength (UTS), Percentage Elongation and other mechanical properties of roofing materials. The corrosion tests were conducted by placing the different samples in five jars containing rain water, sea water, HCl, NaOH and CH_3COOH for 6 days, 16 days, 25 days, 54 days , 60 days, 75 days, 90 days, and 101 days . Surface microstructures of the corroded surfaces were studied using a computer interfaced Optical Microscope (Leica DM 2500M). The corrosion rates per day were also obtained for the samples by formulae. Aluzinc three star galvanized showed the highest Young's Modulus of Elasticity (18 ± 1 MPa), Ultimate Tensile Strength (50 ± 2 MPa) and micro hardness of 3875 ± 9 Nm^{-2}). Average corrosion rates for Aluzinc three star galvanized per day in rain and sea water were 195 ± 67 µg/day and 417 ± 54 µg/day respectively over 101 days, these values were next to those of aluminium in terms of their resistance to corrosion. Aluminium recorded the highest Percentage Elongation of 28 ± 1 %, Breaking Energy of 7,956,600 ± 1542 MJm^{-2} but the least corrosion rate per day in rain and sea water of 121 ± 23 µg/day and 323 ± 10 µg/day respectively over 101 days.

The Ultimate Tensile Strength of Galvanized coated was 43 ± 7 MPa and next to that of Aluzinc three star galvanized and its Percent Elongation of 5 ± 6 % was next to Aluminium. The Ultimate Tensile Strength and Breaking Energy were least for one star galvanized Japan and its corrosion rate per day was next to that of Galvanized Coated in rain and sea water. One star galvanized India recorded the least Young's Modulus of Elasticity of 8 ± 2 MPa and Percentage Elongation of 1 ± 0.1 % but highest corrosion rate per day in rain and sea water. Generally, Aluzinc three star galvanized roofing sheet stood out distinctly as being the overall best material.

TABLE OF CONTENTS

CHAPTER ONE

CHAPTER TWO

CHAPTER THREE

LIST OF TABLES

CHAPTER ONE

INTRODUCTION

1. 1 Brief History of Roofing

Man has utilized various natural resources, technological methods & ways of applications throughout history to create the environmentally safe, effective roofing of today ranging from wood, mud and straw, to tiling, shingles and beyond. A roof can only be as good as the materials readily available, so every civilization had varying methods, tools, and materials for creating their respective roofs. The finished product and the materials used to produce roof are an accurate portrayal of how technologically advanced and creative a certain civilization may have been. Although most of the growth within the roofing industry has been within the last 200 years, the complete history of roofing started much earlier than that.(http://www. Electrospec.ca/lib.pqr.roof.htm, 2010).

The Greeks and Romans were the first to experiment with differing roofing styles. The Romans introduced slating and tiling to Great Britain as early as 100 BC. Thatch roofs were introduced and implemented around the year 735 AD and it wouldn't be for another 300 years until wooden shingles were first implemented as well. It wasn't until the 12th century that the history of roofing was changed forever under King John, when he issued a law in London that citizens had to replace their thatch and reed roof-coverings and replace them with clay tiles. This law was passed as a measure against spreading fires and marked the beginning point for mass-produced, industrial roofing methods.

Dreadnought clay tiles began production in 1805 and industrial roofing at that time had little insulation but a good slope for rainwater and other debris. One hundred year after that, concrete tile roofing was first utilized. While the history of roofing began to evolve, American roofing styles and all of those abroad were still dependent upon the regional availability of materials. In the southern parts of the United States, wood and metal were more widely used. In the Southwest, tile was a lot more prevalent. The Midwest utilized mostly wood roof coverings (Palladio, 1982).

Even to this day, roofing styles are still based around those of local materials, but a wider variety and more expansive materials are now present in many markets throughout the world. Today, materials such as metal sheets, slate, and felt are amongst the most common roofing materials. It is hard to predict the future of the roofing industry and what technology can shape for the future, but for certain, the history of roofing has evolved and will continue to evolve forever (Gilly´en, 1999).

1.2 Metal Roofing

Metal roofing is the most common material used on the roofs in many homes, commercial and industrial premises (Kennedy et al., 2001). Metal roofs come in a number of different forms including long run roofing (corrugated, trapezoidal, trough section/ concealed fix), tile, shakes and flat sheets. Galvanized steel sheet was the most commonly used form of profiled metal roofing prior to the development of zinc/ aluminum alloy coatings. These roofs consist of mild steel coated with zinc. The long run roofing is typically fixed in place using lead-headed nails. Zinc/Aluminum alloy coatings are the most common coating for mild steel roofs. This coating uses zinc 45% and aluminum 55% in the combination to provide sacrificial protection (zinc) and

barrier (aluminum). Zinc/ Aluminium alloy and galvanized coated mild steel are the most commonly used metals for roofs today. Aluminium, stainless steel, copper, lead and zinc can also be used for roofing. With the

exception of Lead, these can be rolled or pressed to form tiles. These materials are usually left unpainted, but can be painted. Materials such as lead have been used traditionally on historical building roof surfaces in European cities. Copper sheets are used to make copper shingles (V´andor, 1999)

1.3 Non Metal Roof Material

Slate roofs include a wide range of geological materials classed as roofing slate. They include asbestos, siltstone, mudstone, shale, marl and limestone asbestos roofs are mainly seen in the form of slates and can be identified by their flaky nature. Clay roofing tiles are gradually becoming more common and do not require additional colouring. In recent times pigment can be added to colour tiles or inorganic oxide coloured cement slurry can be applied to the tile surface by a process known as terracotta. [5]. Concrete tiles are also common in recent times and they are made of sand or Portland cement. They are sometimes covered with a base primer coating which comprises acrylic polymer, pigments, fillers and biocide which forms the top coat. Fibre cement sheets are often used on industrial or commercial buildings. They consist of treated cellulose fibres mixed with cement and sand. They can be used as a replacement for asbestos cement sheet (Pomozi, 1999)

1. 4 Roofing

The slope of a roof is a factor in the life expectancy of the roofing material. The life expectancy of a roof covering is also dependent upon the type of material used, the quality of workmanship, exposure to sun and wear from tree branches, snow/ ice and wind. For example, south and west roof faces have a higher wear factor than north or east exposures, highly reflective shingles tend to have a longer life expectancy, and cement or slate roofs last much longer than metal roofing sheet since they are liable to corrosion but less costly. There are two basic types of roof construction, sloped (also called pictched) and flat.

Sloped roofs are covered with individual pieces of shingling material overlapped to prevent water penetration Other types of covering for sloped roofs include asphalt roll roofing, concrete or clay tiles, wood shakes and shingles, and slate shingles. There are also fiberglass shingles which is more expensive and most Ghanaians cannot afford (V´andor, 1996)

Fig, 1.1 A residential house with sloped roof (V´andor, 1996)

Flat roofs on the other hand are watertight membranes that should have just enough slopes to allow water to run off. Corrugated metal roofing sheets such as One star galvanized, Aluzinc, galvanized coated, Aluminum etc are most commonly used roofing material in residential construction in Ghana. Flat roofs are built up with layers of molten asphalt and felts, or covered with a membrane of modified bitumen or asphalt base, or plastics or rubber. Most are heat-sealed and some are glued (Szab´o, 1999)

Fig. 1.2 Residential house with flat roof (Szab´o, 1999)

1.5 Roof Flashings

The purpose of flashings is to prevent the entry of water at areas on a roof where two components join together or intersect (ie. one roof to another or a chimney through a roof). Flashings can be constructed of galvanized steel, aluminum, copper, lead or lengths of roll-roofing. The choice of flashing material will dependent upon the construction of the roof and the material used for the roof covering.

Flashings will expand and contract particularly in metal roofing sheets such as aluminum, Aluzinc, galvanized coated sheets etc, when heat from the sun and air temperature changes. They are also expected to move and stretch with typical building shifts. In areas where flashings are required are typically very vulnerable to water penetration. There is a high risk of water leakage and wood decay from a damaged, loose or poorly constructed flashing. Due to the above reasons, regular monitoring and routine maintenance of the flashing areas is essential to prevent leakage from the roof to cause corrosion (Schapcot,1999).

1.6 Zinc

Zinc ranks 24th in abundance among the elements in the earth crust. It never occurs free in nature, but is found as zinc oxides (ZnO) in the mineral zincite; as zinc silicate (ZnO.SiO.2H2O), in the mineral franklinite; and as zinc sulphides(ZnS) in the mineral sphalerite, or zinc blend. The ores most commonly used as a source of zinc are 45 smithsonite and sphalerite (Makay, 1999). Zinc has a chemical symbol Zn, with atomic number 30 and relative atomic weight 65.38. It is a member of group (XII) of the periodic table of elements just as cadmium and mercury. It is in period (IV) of the periodic table and in the same period with copper, nickel, manganese and iron. Pure zinc is a crystalline metal, insoluble in hot and cold water but soluble in alcohol, acids and alkalis. It is extremely brittle at ordinary temperatures, but becomes malleable between 120 ºC and 150 ºC (248 F and 302 F) and can be rolled into sheets between heated rollers (Szab´o, 1998). Zinc is unaffected by dry air, in moist air, it is oxidized and becomes coated with a carbonate film that protects it from further corrosion. Zinc melts at about 420 ºC (about 693 F), boils at about 907 ºC (about 1180 F) and has a specific gravity of 7.14. There are five stable isotopes (mass number 64, 66, 67, 68 and 70) and six radioactive isotopes are known.

Chemically, it is a reactive metal, combining with oxygen and other non-metals and reacting with dilute acids to release hydrogen gas.

It also dissolves in alkaline medium to give zincates. Most of its compound contains Zn^{2+} ion. It is amphoteric, forming zincates with bases (Horvath et al,1998). The human body contains between 2 g - 25 g of zinc with three quarters of this amount concentrated in the skeleton. A high concentration of zinc also appears in the skin, hair and testes. In the blood most of the zinc occurs in the red blood cells, platelets and the blood serum. Zinc is found in biological systems only in the +2 valence state. This is due to the extra stability associated with filled d-orbital electronic configuration. Dwarfism related to zinc deficiency has been reported in Turkey, Morocco and Portugal, the United States as well as China [14]. Zinc is nutritionally essential metal and its deficiency can result in a wide spectrum of clinical effects depending on age, stage of development, and deficiencies of related metals. Daily intake 150–600 mg and 6 g are considered toxic and lethal to human. Zinc does not accumulate with exposure, but the body content is modulated by homeostatic mechanisms that principally on absorption and liver levels (Anderson et al, 1976).

1.7 Aluminum

Aluminum is a soft, lightweight metal with a normally dull silvery appearance caused by a thin layer of oxidation that forms quickly when the metal is exposed to air. Aluminum oxide has a higher melting point than pure aluminum. Aluminum has a tensile strength of about 49 MPa in a pure state and 400 MPa as an alloy. Aluminum is about one-third as dense as steel or copper; it is malleable, ductile, and easily machined and cast. It has excellent corrosion resistance and durability because of the protective oxide layer. Aluminum is one of the few metals which retain

full silvery reflectance, even in finely powdered form, which makes it a very important component of silver paints (Larrablee, 1958)

Aluminum is one of the most abundant elements found in the environment. Therefore, human exposure to this metal is common and unavoidable. However, intake is relatively low because this element is highly insoluble in many of its naturally occurring forms. The significance of environmental contact with aluminum is further diminished by the fact that less than 1 % of that taken into the body orally is absorbed from the gastrointestinal tract. The average human intake is estimated to be between 30 and 50 mg per day. This intake comes primarily from foods, drinking water, and pharmaceuticals. Based on the maximum levels reported in drinking water, less than one-fourth of the total intake comes from water

(Humbles. 1994)

1.8 Iron

Metallic iron occurs in the free state and is widely distributed and ranked in abundance among the entire element in the earth's crust, next to aluminum. The principal ore of iron is hermatite, other important ores are goethite, magnetite, siderite and bog iron (Boyd et al,1987). Iron has the chemical symbol Fe; it is a silvery, malleable and ductile metallic transition element with atomic number 26 and relative atomic weight of 55.847. It is in period IV just as arsenic (As), copper (Cu), and Zinc (Zn). Pure iron boils at 27500 ºC (4982ºF) and has a specific gravity of 7.86. Chemically, iron is an active metal which combines with the halogens (fluorine, chlorine, bromine, iodine and astatine) sulfur, phosphorus, carbon, and silicon. It displaces hydrogen from most dilute acids. It burns in oxygen to form ferric oxide, Fe_3O_4 (Reinhart et al, 1992). When

exposed to moist air, iron become corroded forming a reddish-brown, flaky, hydrated ferric oxide commonly known as rust. The formation of rust is an electrochemical phenomenon in which the impurities present in iron form an electrical "couple" with the iron metal. A small current is set up, water from the atmosphere providing an electrolyte in the form of a salt to accelerate the reaction. In this process the iron metal is decomposed and reacts with oxygen in the air to form rust. The reaction proceeds faster in those places where rust accumulates, and the surface of the metal becomes pitted (Malik et al ,1995).

1.9 Aluminum Roofing Sheets

Aluminum corrugated roofing sheets are made of aluminum in its pure state without any alloy. They are widely used in residential house construction and roofing.

Fig. 1. 3 Corrugated Aluminum roofing sheets (Larrabee, 1993)

1.9.1 Specifications of Aluminum Roofing:

(1) Grade: AA1060 ,1070, 1100 ,1200 ,3A21 ,3003

(2) Thickness: 0.3mm-1.5mm

(3) Width: 820mm-1000mm

(4) Temper: H1X H2X

(5) Length: 2000mm, 2500mm, 3000mm, etc.

(6) Paint: PE , PVDF

(7) Color: original aluminum color, Ocean blue, Deep red, Gray, Tephrosious

1.9.2 Features of aluminum roofing

(1) Easy installation   (2) High strength   (3) Low in costs

(4) Durable   (5) Nice appearance   (6) Anti oxidation

1.9.3 Applications for Aluminum Roofing

- Gymnasium

- Warehouse

- Hospital

- Shelter

- Supermarket

- Commercial facilities (Larrabee, 1993)

1.10   Aluzinc Roofing sheets

Aluzinc sheets are obtained by strip immersion at about 610°C in a 600°C bath containing 55 wt.% Aluminum, 43.7 wt.% Zinc and 1.3 wt.% Silicon. Silicon is added to prevent the exothermic Fe/Al reaction to occur by building a Fe-Al-Si-Zn based intermetallic compound and better control coating thickness and formability. Excepted for Fe, coating composition is equivalent to bath composition. Aluzinc coating is thus made of an intermetallic layer and an overlay coating (Hack, 1982).

Fig. 1.4 Different types of aluzinc roofing sheets(Hack, 1982).

1.10.1 Specification of Aluzinc Roof Sheets

- Chemical Composition: 5 5% Aluminum, 43.4% Zinc, 1.6% Silicon

- Standard: JIS3321/ASTM A792M

- Thickness: 0.16mm - 2.0mm

- Width: 600mm - 1250mm

- Aluminum Coating: AZ50/ AZ100/ AZ150/ AZ185

- Spangle: regular spangle, minimized spangle, zero spangle

- Surface treatment: Chemical treatment, oil, dry, anti-finger print

- Color series: RMP/SMP/HDP/PVF2

1.10.2 Features of Aluzinc Roofing Sheet

Long-term resistance to atmospheric corrosion resistance, bright surface, paintability, durable, and versatile.

1.10.3 Applications of Aluzinc oofing Sheet:

Used as the wall or roofing of factories, warehouses, garages, exhibition centers, cinemas etc   (http://www.users.skynet.be/gentec/thrmsel.htm).

1.11 Galvanized Corrugated Steel Roofing sheet

It is a flat rolled steel sheet coated with Zinc Coating Weight of $60 \ g/m^2 - 275 \ g/m^2$ produced by a continuous hot dip process as a result of over 20 years of research.

Fig. 1.5 Galvanized corrugated roofing sheets in different colours(http://www.matweb.com)

1.11.1 Characters of Galvanized Corrugated Steel Roofing sheet

- Excellent waterproof performance

- Durable, anti-corrosion Zinc coating which lasts 20 - 30 years and can withstand bad weather.

- Easy to install, no special tools required.

- Light weight without sacrificing the high strength to weight ratio of steel

- Varieties of colours

1.11.2 Specifications of Galvanized Corrugated Steel Sheet

- Standard: JIS G3302 1998, ASTM A653M/A924M 2004

- Thickness: 0.13 mm - 0.5 mm

- Width: 400 mm – 1000 mm

- According to customers specification

- Zinc Coating Weight: 60 g/m^2 – 275 g/m^2

- Raw Materials: Galvanized steel sheet and Pre-painted galvanized steel sheet

- Spangle: Regular spangle, minimized spangle and zero spangle

- Hardness: Full hard, normal

1.11.3 Applications of Galvanized Corrugated Steel Sheet

Used as wall or roofing for factories, warehouses, garages, exhibition centers, cinemas, etc

 [http://www.matweb.com]

1.12 Objectives of the project

The objective of this project is to study the tensile strength, micro hardness and corrosion effect on some selected roofing sheets in the building industry in the Ghanaian market. Usually routine checks like tensile test, micro hardness test, corrosion and surface microstructure studies are carried out to establish whether the different products of metal roofing sheets meets the required specification. These tests are carried out to establish the relationship between the tensile strength, micro hardness and corrosion effects of the metal sheets. Since there are different types of roofing sheets in the country, the choice of roofing material with long life span will depend on these properties.

1.13 Justification of the Project

There is high demand for accommodation in the country and choice of long lasting roofing sheet is very important as the roof plays a major role in building construction. Due to the high demand for roofing sheets, the local industries (Tema Aluworks and other industries) unable to meet the demand hence the need to import from other countries such as Japan, China, India etc. The imported roofing materials are in the form of bundle and are cut into thickness of 0.3mm-1.5mm, Width of 820mm -1000mm and Length of 2000mm, 2500mm, 3000mm, etc before corrugation is made on the sheets by the local industries . The roofing sheets are branded by the local industries as One star galvanized coated Japan[G1*Jap], Galvanized coated [GC], three star aluzinc galvanized [AlZn3*], one star galvanized India [G1*Ind], aluminum roofing sheets etc . This project seeks to study the tensile strength, micro hardness and corrosion effect of the locally produced roofing sheets and some of the imported roofing sheets in the building industry.
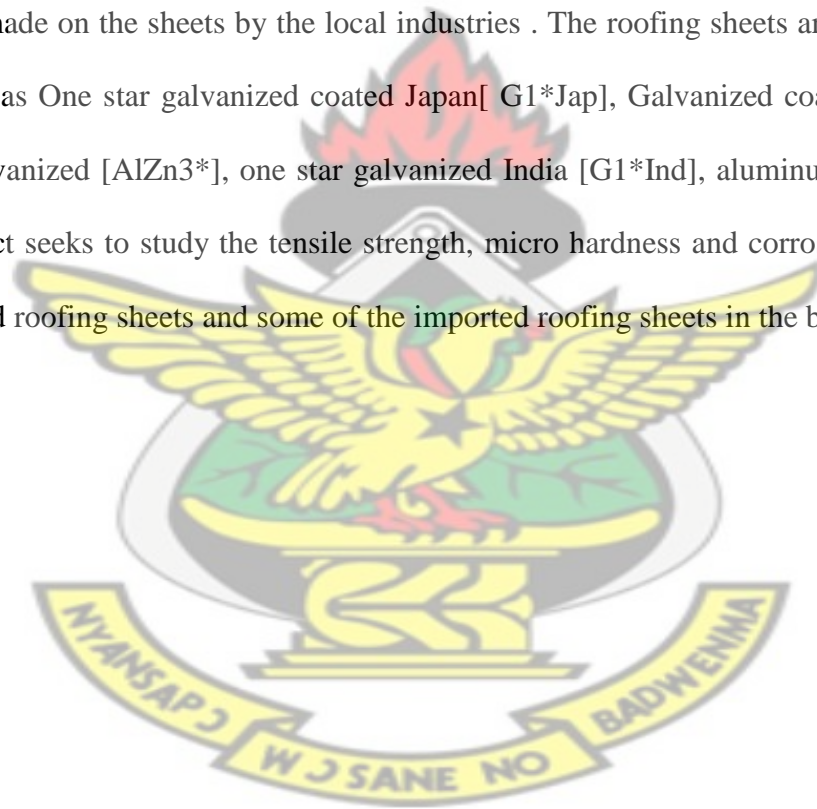
CHAPTER TWO

LITERATURE REVIEW

2.1 Introduction to tensile testing

Tensile tests are performed for several reasons and the results of tensile tests are used in selecting materials for engineering applications. Tensile properties frequently are included in material specifications to ensure quality and are often measured during development of new materials and processes, so that different materials and processes can be compared. Finally, tensile properties often are used to predict the behavior of a material under forms of loading other than uniaxial tension. The strength of a material may be measured in terms of either the stress necessary to cause appreciable plastic deformation or the maximum stress that the material can withstand. These measures of strength are used, with appropriate caution (in the form of safety factors), in engineering design (Oldfield et al,1997)

Low ductility in a tensile test is accompanied by low resistance to fracture under other forms of loading. Elastic properties also may be of interest, but special techniques must be used to measure these properties during tensile testing, and more accurate measurements can be made by ultrasonic techniques. This chapter provides a brief overview of some of the more important topics associated with tensile testing. These include: stress-strain curves, including discussions of elastic versus plastic deformation, yield points, and ductility, true stress and strain, test methodology and data analysis (Malik et al, 1997)

2.2 Tensile test

Tensile properties indicate how the material will react to forces being applied in tension. It measures the force required to pull something such as rope, wire, or a structural beam to the point where it breaks. It is measured in units of force per unit area. In the SI system, the units are Newton per square meter or Pascal. Specially, the tensile strength of a material is the maximum amount of tensile stress that it can be subjected to before failure. The definition of failure can vary according to material type and design methodology. This is an important concept in engineering, especially in the fields of materials science, material engineering and structural engineering. A tensile test is a fundamental mechanical test where a carefully prepared specimen is loaded in a very controlled manner while measuring the applied load and the elongation of the specimen over some distance. Tensile tests are used to determine the Tensile Strength, Toughness, and Modulus of Elasticity, Elastic Limit, Percentage Elongation, Yield Point and other tensile properties (Larrabee, 1999).

Tensile Strength is an intensive property and, consequently, does not depend on the size of the test specimen. However, it is dependent on the preparation of the specimen and the temperature of the test environment and material (Hack, 1982).

2.2.1 Stress-Strain Diagrams

The internal resistance of the material to counteract the applied load is called stress, and the deformation as strain. There are three types of stresses:

- **Tensile stress:** force acts to pull materials apart
- **Compressive stress:** the force squeezes material

- **Shear stress:** the force causes one part to slide on another part

2.2.2 Principal Mechanical Properties

The characteristics of materials which describe their behavior under external loads are known as mechanical properties. The most important and useful mechanical properties are:

❖ **Strength:** It is the resistance offered by a material when subjected to external loading. Hence the stronger the material the greater the load it can withstand. Depending upon the type of load applied the strength can be tensile, compressive, shear or tensional.

❖ **Elasticity:** Elasticity of a material is its power of coming back to its original position after deformation when the stress or load is removed. Elasticity is a tensile property of its material. The greatest stress that a material can endure without taking up some permanent set is called elastic limit (Rao, 2011).

❖ **Plasticity:** The plasticity of a material is its ability to undergo some degree of permanent deformation without failure. Plastic deformation will take place only after the elastic range has been exceeded. Plasticity is an important property and widely used in several mechanical processes like forming, shaping, extruding and many other hot and cold working processes. In general, plasticity increases with increasing temperature and is a favorable property of material for secondary forming processes. Due to these properties various metals can be transformed into different products of required shape and size. This conversion into desired shape and size is effected either by the application of pressure, heat or both (Rao, 2011).

❖ **Ductility:** Ductility is the property of a material that enables it to be drawn into thin wire on application of the load. Mild steel is a ductile material. The wires of gold, silver, copper, aluminum, etc. are drawn by extrusion or by pulling through a hole in a die due to the ductile property. The ductility decreases with increase of temperature. The percentage elongation and the reduction in area in tension are often used as empirical measures of ductility.

❖ **Malleability:** Malleability of a material is its ability to be flattened into sheets without cracking by hot or cold working. Aluminum, copper, tin, lead, steel, etc. are malleable metals. Lead can be readily rolled and hammered into thin sheets but cannot be drawn into wire. Ductility is a tensile property, whereas malleability is a compressive property. Malleability increases with increase of temperature (Rao, 2011).

❖ **Brittleness:** The brittleness of a material is the property of breaking without much permanent distortion. There are many materials, which break or fail before much deformation takes place. Such materials are brittle e.g., glass, cast iron. Therefore, a non-ductile material is said to be a brittle material. Usually the tensile strength of brittle materials is only a fraction of their compressive strength. A brittle material should not be considered as lacking in strength. It only shows the lack of plasticity and on stress-strain diagram these materials don't have yield point and value of Young's modulus of elasticity is small (Rao, 2011)..

❖ **Toughness:** The toughness of a material is its ability to withstand both plastic and elastic deformations. It is a highly desirable quality for structural and machine parts to withstand shock and vibration. Manganese steel, wrought iron, mild steels are tough materials. For example if a load is suddenly applied to a piece of mild steel and then to a piece of glass the mild steel will absorb much more energy before failure occurs. Thus, mild steel is said to be much tougher than a glass. Toughness is a measure of the amount of energy a material can absorb before actual fracture.

"The work or energy a material absorbs is called modulus of toughness" (Rao,2011).

2.2.3 Some typical definitions of tensile properties

▪ **Yield strength:** The stress at which a material strain changes from elastic deformation to plastic deformation, causing it to deform permanently.

▪ **Ultimate Tensile strength (UTS):** The maximum stress a material can withstand when subjected to tension, compression or shearing. It is the maximum stress on the stress - strain curve.

▪ **Breaking strength:** The stress coordinates on the stress - strain curve at the point of rupture.

▪ **Offset Yield Strength (OYS)** : Represents a point just beyond the onset of permanent deformation

▪ **Rupture (R) or Fracture point:** Separation of specimen into pieces (Boyd et al, 1999)

The various definitions of tensile are shown in the following stress-strain graph.

● **Modulus of Elasticity:** This is a measure of the stiffness of the material, but it only applies in the linear region of the curve. If a specimen is loaded within this linear region, the material will return to its exact same condition if the load is removed. At the point that the curve is no longer

linear and deviates from the straight-line relationship, Hooke's Law no longer applies and some

permanent deformation occurs in the specimen. This point is called the "elastic, or proportional,

limit". From this point on in the tensile test, the material reacts plastically to any further increase

in load or stress. It will not return to its original, unstressed condition if the load were removed (

Reinhart et al, 1993)
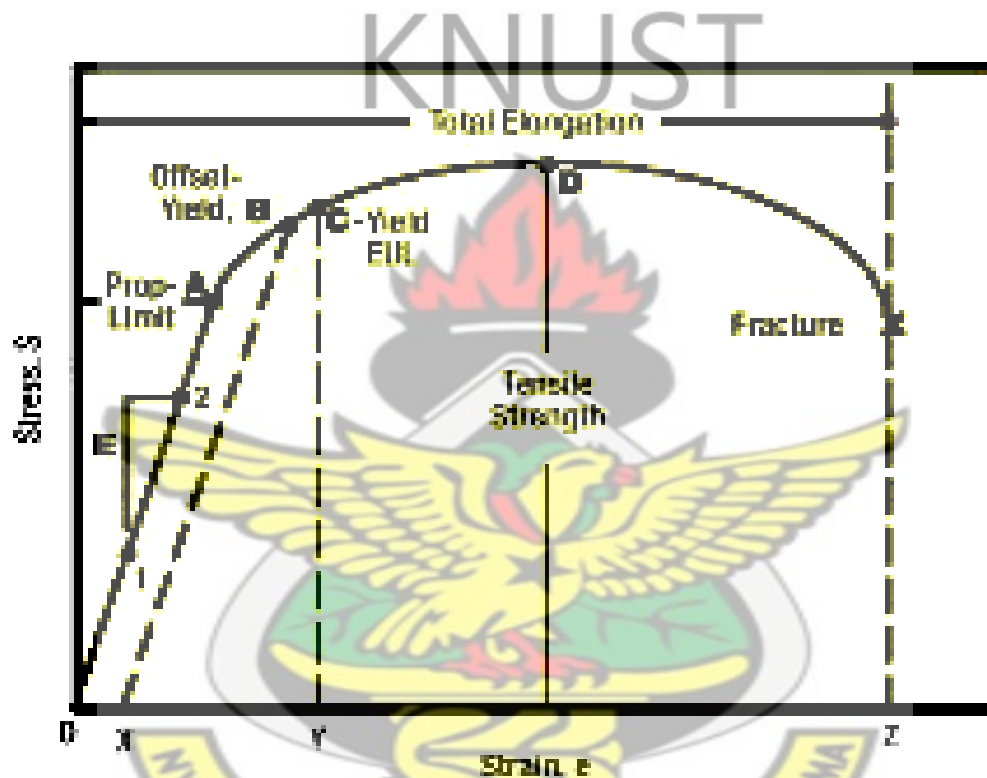
Fig.2.1 An engineering stress vrs strain curve (Oldfield et al, 2000)

Fig. 2.1 shows the stress-strain diagram with values of stress (load) as ordinate and strain

(elongation, compression, deflection, twist etc.) as abscissa. Mechanical properties depend upon

the crystal structure, its bonding forces, and the imperfections which exist within the crystal. The

shape and magnitude of the curve is dependent on the type of metal being tested. Point A

represents the proportional limit of a material. A material loaded in tension beyond point A when

unloaded will exhibit permanent deformation. The proportional limit is often difficult to

calculate, therefore, two practical measurements, offset yield strength (OYS) and yield by extension under load (EUL) were developed to approximate the proportional limit. The initial portion of the curve below point A represents the elastic region and is approximated by a straight line. The slope (E) of the curve in the elastic region is defined as Young's Modulus of Elasticity and is a measure of material stiffness (Oldfield et al, 2000).

Point B represents the offset yield strength and is found by constructing a line X-B parallel to the curve in the elastic region. Line X-B is offset a strain amount O-X that is typically 0.2% of the gage length. Point C represents the yield strength by extension under load (EUL) and is found by constructing a vertical line Y-C. Line Y-C is offset a strain amount O-Y that is typically 0.5% of gage length. The ultimate tensile strength, or peak stress, is represented by point D. Total elongation, which includes both elastic and plastic deformation, is the amount of uniaxial strain at fracture and is depicted as strain at point Z. Percent Elongation at break is determined by removing the fractured specimen from the grips; fitting the broken ends together and measuring the distance between gage marks. Percent elongation at break reports the amount of plastic deformation only.

Reduction of area, like elongation at break, is a measure of ductility and is expressed in percent. Reduction of area is calculated by measuring the cross sectional area at the fracture point (Az) (Oldfield et al, 2000).

2.3 Hardness Test

Hardness is the property of a material that enables it to resist deformation, however, is not an intrinsic material property dictated by precise definitions in terms of fundamental units of mass, length, and time. A hardness property value is the result of a defined measurement procedure.

Hardness tests characterize the materials and determine if they are suitable for their intended use. All of the hardness tests described in this section involve the use of a specifically shaped indenter, significantly harder than the test sample. The indenter is pressed into the surface of the sample using a specific force. Either the depth or size of the indent is measured to determine a hardness value. Establishing a correlation between the hardness result and the desired material property makes hardness tests useful in industrial applications (Malik et al, 2005).

Four major hardness tests described are as follows (Malik et al, 2005).

 (1) Rockwell test

 (2) Brinell test

 (3) Vickers test

 (4) Micro hardness (Knoops test)

Each of these tests uses a specifically shaped diamond indenter, made from carbide or hardened steel. The indenter is pressed into the material with a specific force using a defined test procedure. The hardness values are determined by measuring either the depth of indenter penetration or the size of the resultant indent and compared with hard scales.

Current methods such as Rockwell or Brinell, use a minimum load of approximately 5 grams force (gf). However, the resulting indentation may be too large for thin film coating, and the underlying layer interferes with accurate hardness measurement. Therefore, an ultra-low load hardness test, a micro hardness test was developed for thin metal sheets(Malik et al, 2005)..

2.3.1 Rockwell Test

The Rockwell test method is the most commonly used hardness test method, since it is easier to perform and more accurate than other types. Rockwell is used on all metals except where the test

metal structure or surface conditions introduce too much variation, where the indentations is too large for the application, or where the sample size or shape prohibits its use. The Rockwell hardness test measures the depth of indentation produced by the preliminary and total test forces. First, a preliminary test force is applied; this is the zero or reference position. Next, an additional test force is applied to reach the total required test force. This additional force is held for a predetermined amount of time and released, but the preliminary test force still applied. The indenter reaches the final position at the preliminary force and the distance traveled from the major load position is measured and converted to a hardness number (Malik et al, 2005).

2.3.2 Brinell Test

The Brinell hardness test method consists of indenting the test material with a hardened steel or carbide ball. The diameter of the indentation left in the test material is measured with a low powered microscope. The Brinell hardness number is calculated by dividing the load applied by the surface area of the indentation. Compared to the other hardness test methods, the Brinell ball makes the deepest and widest indentation, so the test averages the hardness over a wider amount of material, which will more accurately account for multiple grain structures and any irregularities in the uniformity of the material (Malik et al, 2005).

The Brinell method is the best for achieving the bulk or macro-hardness of materials with heterogeneous structures. Some applications where the Brinell hardness test is used are the following:

• Forgings/castings

• Heavy truck/bulldozer parts

• Engine blocks and heads

• Non-homogeneous materials

• Rear-end housings

• Springs

• Variety of large, coarse-surface parts (Malik et al, 2005).

2.3.3 Vickers Test

In the Vickers hardness test method, the indenter is a right pyramid with a square base and an angle of 136 degrees between opposite faces. The two diagonals of the indentation left in the surface of the material after removal of the load are measured using a microscope and their average calculated. The area of the sloping surface of the indentation is calculated. The Vickers hardness is the quotient obtained by dividing the kgf load by the square millimeter area of indentation.

The Vickers test has two force ranges from micro (10 to 1000 g) to macro (1 to 100 kg) . The indenter is the same for both ranges, and the Vickers hardness values are continuous over the total range of hardness for metals (typically HV100 to HV1000). The advantages of the Vickers hardness test are that extremely accurate readings can be taken, and only one type of indenter used for all types of metals and surface treatments. Because of the wide test force range, the Vickers test can be used on almost any metallic material (Malik et al, 2005).

2.3.4 Knoops Test

The Micro hardness test method specifies a range of loads using a diamond indenter to make an indentation that is measured and converted to a hardness value.

There are two types of micro hardness indenters and these are:

  (i) a square base pyramid shaped diamond used in a Vickers tester

  (ii) and a narrow rhombus shaped indenter for a Knoop tester.

Typically, loads are very light, ranging from a few grams to one or several kilograms. The term micro hardness refers to static indentations made with loads not exceeding 1 kgf.

The procedure for testing is very similar to that of the standard Vickers hardness test, except that it is done on a microscopic scale with higher precision instruments. Precision microscopes used to measure the indentations, have a magnification of approximately X500, and measure an accuracy of +0.5 micrometers. Like the Vickers test, the Knoop micro hardness test has a wide test force range, and it can be used on almost any metallic material. The primary application of the micro hardness test is measuring the hardness of a thin film coating(Malik et al, 2005).

2.4 Corrosion

2.4.1 Definition of Corrosion

Corrosion is the destruction of materials caused by chemical or electrochemical action of the surrounding environment. This phenomenon is experienced in day to day living. The most common examples of corrosion include rusting, discoloration and tarnishing. Corrosion is an ever occurring material disease which can only be reduced but not prevented because thermodynamically it is a spontaneous phenomenon. Oxygen, biological activities, pollution,

temperature, salinity and velocity are the major factors which affect the corrosion behavior of roofing sheets (Hack, 2006).

2.4.2 Types of corrosion

2.4.2.1 Concentration Cell Corrosion

Concentration cell corrosion occurs when two or more areas of a metal roof surface are in contact with different concentrations of the same solution.

The three general types of concentration cell corrosion are:

(i) **Metal ion concentration cells**

In the presence of water, a high concentration of metal ions will exist under faying surfaces and low concentrations of metal ions exist adjacent to the crevice created by the faying surfaces. An electrical potential will exist between the two points. The area of the metal in contact with the low concentration of metal ions will be the cathode and protected, and the area of metal in contact with the high metal ion concentration will also be anodic which will corrode(Hack, 2006).

(ii) **Oxygen concentration cells**

Water solution in contact with the metal roof surface will normally contain dissolved oxygen. An oxygen cell develops at a point where oxygen in air is not allowed to diffuse uniformly into the solution, thereby creating a difference in oxygen concentration between two points. Typical locations of oxygen concentration cells occur under metallic or nonmetallic deposits (dirt) on the metal roof surface and under faying surfaces such as riveted lap joints (Hack, 2006)..

(iii) **Active passive cells**

Metals that depend on a tightly adhering passive film (usually an oxide) for corrosion protection; e.g., austenitic corrosion-resistant steel, can be corroded by active-passive cells. The corrosive action usually starts as an oxygen concentration cell; e.g., salt deposits on the metal roof surface in the presence of water containing oxygen creates the oxygen cell. If the passive film is broken beneath the salt deposit, the active metal beneath the film is exposed to corrosive attack. An electrical potential develops between the large area of the cathode (passive film) and the small area of the anode (active metal). Rapid pitting of the active metal will result (Hack, 2006)

2.4.2.2 Galvanic Corrosion

Galvanic corrosion is an electrochemical action of two dissimilar metals which are in contact. in the presence of an electrolyte and an electron conductive path. It is recognizable by the presence of a buildup of corrosion at the joint between the dissimilar metals.

For example, when aluminum alloys or magnesium alloys are in contact with steel (carbon steel or stainless steel), galvanic corrosion occur (Hack, 2006).

2.4.2.3 Intergranular Corrosion

Intergranular corrosion is an attack on the grain boundaries of a metal or alloy. This structure consists of quantities of individual grains; each of these tiny grains has a clearly defined boundary that chemically differs from the metal within the grain center. Frequently, the grain boundaries are anodic to the main body of the grain, and when the grain boundaries are in this

condition and in contact with an electrolyte, a rapid selective corrosion of the grain boundaries occurs. An example of intergranular or grain boundary corrosion is one which occurs when aluminum alloys are in contact with steel in the presence of an electrolyte. The aluminum alloy grain boundaries are anodic to both the aluminum alloy grain and the steel. In the later case, intergranular corrosion of the aluminum alloy occurs Hack, 2006).

2.4.2.4 Pitting Corrosion

The most common effect of corrosion on aluminum and magnesium alloys is called pitting. It is noticeable first as a white or gray powdery deposit, similar to dust, which blotches the surface. When the deposit is cleaned away, tiny pits or holes can be seen in the surface of the roofing sheet. Passive metals such as stainless steel resist corrosive media and can perform well over long periods of time. However, if corrosion does occur, it forms at random in pits. Pitting may be a serious type of corrosion because it tends to penetrate rapidly into the metal section. Pits begin by a breakdown of passivity at nuclei on the metal surface. The breakdown is followed by formation of an electrolytic cell, the anode of which is a minute area of active metal and the cathode of which is a considerable area of passive metal. Pitting is most likely to occur in the presence of chloride ions, combined with such depolarizers as oxygen or oxidizing salts (Hack, 2006).

2.4.2.5 Uniform Etch Corrosion

The surface effect produced by most direct chemical attacks (e.g. acid or base) is a uniform etching of the metal. On a polished surface, this type of corrosion is first seen as a general dulling of the surface and, if allowed to continue, the surface becomes rough and possibly frosted

in appearance. The use of chemical-resistant protective coatings or more resistant materials will control these problems (Hack, 2006).

2.4.2.6 Stress Corrosion Cracking

Stress corrosion cracking (SCC) is caused by the simultaneous effects of tensile stress and corrosion. Stress may be internally or externally applied. Internal stresses are produced by non uniform deformation during cold working, by unequal cooling from high temperatures, and by internal structural rearrangement involving volume changes. The magnitude of the stress varies from point to point within the metal. Stresses in the neighborhood of the yield strength are generally necessary to promote SCC, but failures have occurred at lower stresses (Hack, 2006).

2.4.2.7 Fatigue Corrosion

Fatigue corrosion is a special case of stress corrosion caused by the combined effects of cyclic stress and corrosion. No metal is immune from some reduction of its resistance to cyclic stressing if the metal is in a corrosive environment. Damage from fatigue corrosion is greater than the sum of the damage from both cyclic stresses and corrosion. Fatigue corrosion failure occurs in two stages. During the first stage, the combined action of corrosion and cyclic stresses damages the metal by pitting and crack formation to such a degree that fracture by cyclic stressing will ultimately occur, even if the corrosive environment is completely removed. The second stage is essentially a fatigue stage in which failure proceeds by propagation of the crack and is controlled primarily by stress concentration effects and the physical properties of the metal (Hack, 2006)..

2.4.2.8 Fretting Corrosion

The rapid corrosion that occurs at the interface between contacting, highly loaded metal surfaces when subjected to slight vibratory motions is known as fretting corrosion. This type of corrosion is most common in bearing surfaces in machinery, such as connecting rods, splined shafts, and bearing supports, and often causes a fatigue failure. It can occur in structural members such as trusses where highly loaded bolts are used and some relative motion occurs between the bolted members. Fretting corrosion is greatly retarded when the contacting surfaces can be well lubricated as in machinery-bearing surfaces so as to exclude direct contact with air (Hack, 2006).

2.4.2.9 Crevice Corrosion

Contact or crevice corrosion occurs when surfaces of metals are used in contact with each other or with other materials and the surfaces are wetted by the corrosive medium or when a crack or crevice is permitted to exist in a stainless-steel part exposed to corrosive media (Hack, 2006).

2.5 Corrosion Resistance

When left unprotected, steel will corrode in almost any environment. Zinc coatings protect steel by providing a physical barrier as well as cathodic protection for the underlying steel. It is important that the correct zinc coating is specified to provide optimal performance under the exposure conditions to which the coating will be subjected (LaQue, 2005).

2.5.1 Barrier Protection

Zinc coatings provide a continuous, impervious metallic barrier that does not allow moisture to contact the steel. Without moisture, there is no corrosion, except in certain chemical atmospheres. The effectiveness of zinc coatings in any given environment is directly

proportional to coating thickness. Coating life is determined by the coating corrosion rate, itself a function of many factors such as time, composition of the atmosphere and the type of coating. In situations of outdoor exposure, the acidity level of rain will influence the zinc corrosion rate. With indoor exposure - ventilation ducts, floor decks and steel framing, for example - moisture may also be present. In industrial indoor situations, the atmosphere may be corrosive. Thus the type and weight of coating required depends both on the service life needed and the exposure conditions. Corrosion resistance of coatings can also be improved by using a zinc alloy coating, such as Galfan or Galvalume, or by applying paint top coats. These two methods, individually or together, are recommended for exposed sheet applications where enhanced corrosion protection is required (LaQue, 2005).

2.5.2 Cathodic Protection

Another outstanding protection mechanism is zinc's remarkable ability to galvanically protect steel. When base steel is exposed, such as at a cut edge or scratch, the steel is catholically protected by the sacrificial corrosion of the zinc coating adjacent to the steel. In practice, this means that a zinc coating is not undercut because the steel cannot corrode adjacent to a zinc coating. This contrasts with paint and aluminum coatings where the corroding steel progressively undercuts the surrounding barrier film. The extent of this cathodic protection is determined by the type of coating, its thickness and that of the underlying steel, as well as by the area of damage (LaQue, 2005).

2.5.3 Painted Zinc Coatings

Zinc coatings are easily painted. The term "duplex coating" is used for galvanized and painted steel parts, whereas the term "coil coating" or "pre-painting" is used for continuous galvanized and painted steel sheet. Paint acts as a barrier protecting the underlying zinc coating. Zinc is an excellent substrate for paint coatings because if the paint film is broken, zinc's high corrosion resistance prevents undercutting of the paint film. Even if the coating damage does reach the steel base, zinc's cathodic action will prevent the steel from corroding. Zinc's ability to extend the life of paint coatings is what makes pre-painted galvanized steel sheet such a durable product that continues to extend its market share in commercial and residential roofing and cladding applications (Boyd and Fink, 2006).

2.6 Effect of Seawater Level on Corrosion Behavior of Roofing Sheets

Seawater is one of the most corrosive and abundant naturally occurring electrolytes. The corrosively of the seawater is reflected by the fact that most roofing sheets are attacked by this liquid or its surrounding environments. Oxygen, acidity of solutions, biological activities, pollution, temperature, and salinity are the major factors that affect the corrosion behavior of roofing sheets (Hart, 2009).

2. 7 Hydrochloric Acid

Hydrochloric acid is a clear, colorless solution of hydrogen chloride (HCl) in water. It is a highly corrosive, strong mineral acid with many industrial uses. Hydrochloric acid is found naturally in gastric acid. Hydrochloric acid was produced from vitriol (sulfuric acid) and common salt. With major production starting in the Industrial Revolution, hydrochloric acid is used in the chemical industry as a chemical reagent in the large-scale production of vinyl chloride for PVC plastic. HCl has numerous smaller-scale applications, including household cleaning, production of gelatin and other food additives, descaling, and leather processing.

Hydrogen chloride (HCl) is a monophonic acid, which means it can dissociate (i.e., ionize) only once to give up one H^+ ion (a single proton). In aqueous hydrochloric acid, the H^+ joins a water molecule to form a hydronium ion, H_3O^+ (Oldfield and Todd, 2009)

$$HCl + H_2O \rightarrow H_3O^+ + Cl^- \qquad\qquad 2.1$$

The other ion formed is Cl^-, the chloride ion. Hydrochloric acid can therefore be used to prepare salts called chlorides, such as sodium chloride and it is a strong acid, since it is essentially completely dissociates in water. When chloride salts such as NaCl are added to aqueous HCl they have practically no effect on pH, indicating that Cl^- is an exceedingly weak conjugate base and that HCl is fully dissociated in aqueous solution (Oldfield and Todd, 2009).

Of the six common strong mineral acids in chemistry, hydrochloric acid is the monoprotic acid least likely to undergo an interfering oxidation-reduction reaction. It is one of the least hazardous strong acids to handle; despite its acidity, it consists of the non-reactive and non-toxic chloride ion. Intermediate-strength hydrochloric acid solutions are quite stable upon storage, maintaining their concentrations over time. These attributes, plus the fact that it is available as a pure reagent, make hydrochloric acid an excellent acidifying reagent.

Hydrochloric acid is frequently used in chemical analysis to prepare ("digest") samples for analysis. Concentrated hydrochloric acid dissolves many metals and forms oxidized metal chlorides and hydrogen gas, and it reacts with basic compounds such as calcium carbonate or copper (II) oxide, forming the dissolved chlorides that can be analyzed (Oldfield and Todd, 2009).

2. 8 Rain Water

In general, unpolluted rain water has a pH less than 6, which is slightly acidic. This is due to naturally occurring carbon dioxide in the atmosphere reacting with the water vapour to lower pH. Rain water can become more acidic when it is affected by certain atmospheric conditions, industrial fallout and even rainfall intensity and frequency. Acid rain can occur in industrial and heavily polluted areas with fumes from motor vehicle exhaust are more corrosive to roofing sheets than unpolluted rain water. Rain water near the coastal areas can pick up chlorides from salt air due to turbulence of the surf prior to precipitation, and overnight condensation can be similarly affected.

Harvested rainwater can be used in several ways. If the water quality is controlled, it can be used as drinking water. Other domestic uses such as cooking, washing and cleaning are also possible. Moreover, rainwater can be used to keep sanitation facilities clean and hygienical. Beside domestic uses, rainwater can also be used to improve (small scale) agriculture, cattle breeding and even small scale industries (Humbles, 2009).
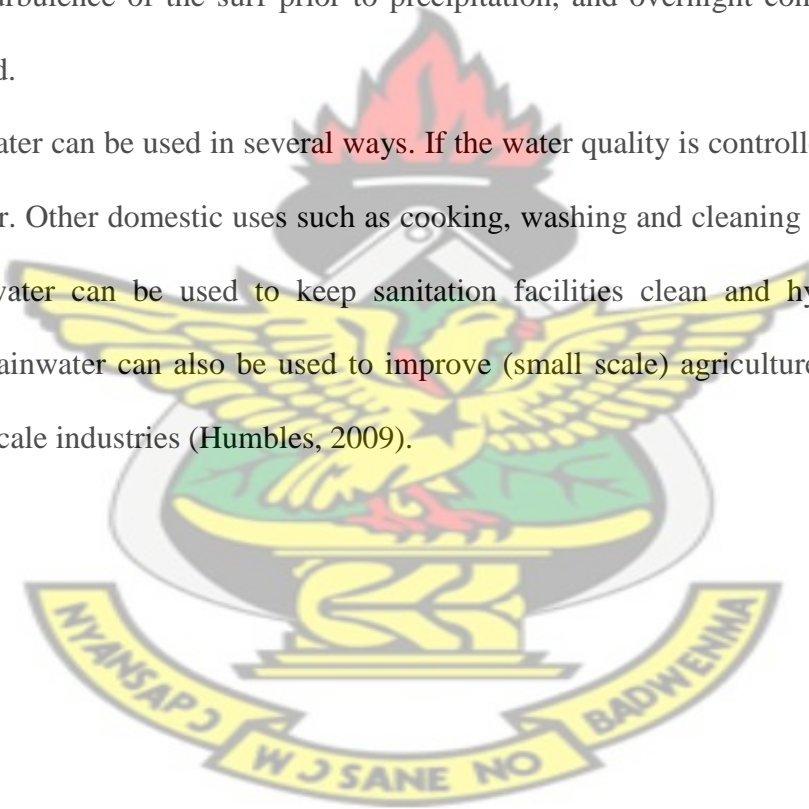
CHAPTER THREE

EXPERIMENTAL DETAILS

3.1 Introduction

The various metal roofing sheets investigated were obtained from Donyma Steel Works Kumasi, These are One-star galvanized roofing sheet (Japan) [G1*Jap], Galvanized coated [GC], Aluzinc three star galvanized [AlZn3*], One star galvanized (India) [G1*Ind] and Aluminum sheet [Al] were cut with scissors into dimensions of 2 cm x 5 cm corrosion analysis and 5 cm x 5 cm for the micro hardness analysis and 2 cm x 25 cm for tensile tests.

Table 3.1   Sample codes and description

Sample Name	Code
One star galvanized sheet (Japan)	G1*Jap
Galvanized coated sheet	GC
Aluzinc three star galvanized	AlZn3*
One star galvanized (India)	G1*Ind
Aluminum	Al

3.2 Corrosion Tests

Roofing sheets for corrosion tests were cut into dimension of 5 cm x 2 cm with holes drilled at one end of the roofing sheet (Fig 3.1) and suspended by means of a nylon thread in each of the solutions. Initial mass of each roofing sheet was measured and recorded as m (t_o). Twenty-five glass jars were used to hold 0.5 M sodium hydroxide solution, 0.2 M hydrochloric acid solution, 0.5 M acetic acid solution, sea water and rain water. The pH of each solution was measured at the start of the experiment and each glass jar covered with a lid to prevent evaporation of solution over time. The corrosion samples (roofing sheets) were removed from each glass jar after 6 days, 16 days, 25 days, 54 days , 60 days, 75 days, 90 days, and 101 days to determine change in colour, shape and mass [m (t)]. Each time the roofing samples were brought out of the solutions, they were washed with distilled water, rinsed in ethanol to stop the reaction, dried and weighed to determine the mass losses. Equation 3.2 was used to calculate the corrosion rate per day. The roofing samples were further subjected to surface metallographic studies using the Leica DM 2500M optical reflection microscope.

Gravimetric analysis prior to corrosion tests were determined to get mass loss, Δm (g), with respect to the initial and final mass after each specified period.

$$\Delta m = m(t_0) - m\ (t) \dots\dots\dots\dots\dots\dots\dots\dots\dots\dots\dots\dots\dots3.1$$

Corrosion rate (CR) for each sample was calculated as follows:

$$CR = \frac{\Delta m}{(t - t_0)A} \quad \dots\ \dots\dots\dots\dots\dots\dots\dots\dots\dots\dots3.2$$

Where t_o = initial time at the start of experiment$\dots\dots\dots\dots\dots\dots\dots.\dots3.3$

t = time after 6 days, 25 days, 54 days , 60 days, 75 days, 90 days, and 101 days   3.4

A = area of each roofing s sheet after each specified period of time   3.5

Graphs showing the corrosion rate per day for 101 days are shown in Fig. 4.1 - 4.2

(a)

(b)

(c)

(d)

(e)

Fig. 3.1 Prepared samples for corrosion tests (a) GC (b) G1*Jap (c) AlZn3*(d) G1*Ind (e) Al

3.2.1 Preparation of Sampling Containers

In order to obtain accurate results, procedures were adopted to eliminate or minimize potential contamination of the samples. Sample containers were soaked in nitric acid overnight and were rinsed with de-ionized water and dried. Some of the dried containers were selected, filled with distilled water and the pH measured ; when it was between 6 to 7 then it was ready for use, otherwise the sampling container was washed again and the pH measured once more. Sample containers were labeled for easy identification.

3.2.2 Collection of Rain Water

Rainwater was collected directly from the skies in an open environment. The samples were collected ten minutes after the start of the rain into one liter (1L) acid leached polythene containers. This was done to minimize pollution due to atmospheric sources and the pH was immediately measured.

3.2.3 Collection of Sea Water

Seawater was collected directly from the sea at New Takoradi beach into one liter (1L) polythene containers and the pH immediately measured using pH indicator.

3.2.4 pH Measurement

After collection of rain and sea water, the pH test strip was opened and without spilling the samples, the pH test strip was placed in it so that the end with the coloured test pads were completely in the water sample. The test strip was slowly moved back and forth motion for 10 seconds, removed from the sample and shaken off to remove excess water. It was then laid flat on the table with the colored pads facing up for 20 seconds to allow the color to develop. The

colour was compared with that on the pH test strip colour chart. The pad on the left strip was matched with the colour on the left, and the pad on the right with the color it is most like in the column on the right. The pH value for the colours closest to the test strip was noted. The pH value between 0 to 6 shows acidity, 7 is neutral and 8 to 14 shows basic solution.

3.2.5 Calculation of Molarity

Equation 3.3 below shows the formula used to calculate the molarities of various solutions for corrosion tests.

$$\text{Mass of conc. solution weighed} = \frac{(\text{no. of moles of conc.solution}) - (1\,mL\ of\ conc.solution)}{\text{no. of moles contained in 1 mL conc.solution}} \ \dots\dots 3.3$$

3.2.5.1 Preparation of 0.5 M Sodium Hydroxide (NaOH) Solution

An amount of 19.95 g sodium hydroxide pellets was weighed and dissolved in 500 ml distilled water in a volumetric flask where it completely dissolves. Water was added until the volume of the solution was 1000 ml.

3.2.5.2 Preparation of 0.5 M acetic (CH_3COOH)acid solution

11.49 ml solution of concentrated CH_3COOH was added to a 500 ml of distilled water in a volumetric flask. To this mixture was added more distilled water until it got to the 1000 ml mark.

3.2.5.3 Preparation of 0.2 M of HCl Acid Solution

4.16mL solution of concentrated Hydrochloric acid was added to a 500mL of distilled water in a volumetric flask. To this mixture was added more distilled water until it got to the 1000mL mark.

(a)

(b)

(c)

(d)

Fig.3.2 various samples suspended in (a) rain water (b) sea water (c) 0.5 M sodium hydroxide solution (d) 0.5 M acetic acid solution (e) 0.2 M Hydrochloric acid solution for corrosion test

The corroded roofing samples were placed on a slide on plasticine one after the other, leveled and placed under the microscope. Magnification (5X) was chosen by selecting one of the objective pieces. The focusing ring was adjusted until a good focus was found by looking into the eye piece lens. The image of the microstructure was projected on a monitor of a computer as shown in Fig.3.3.
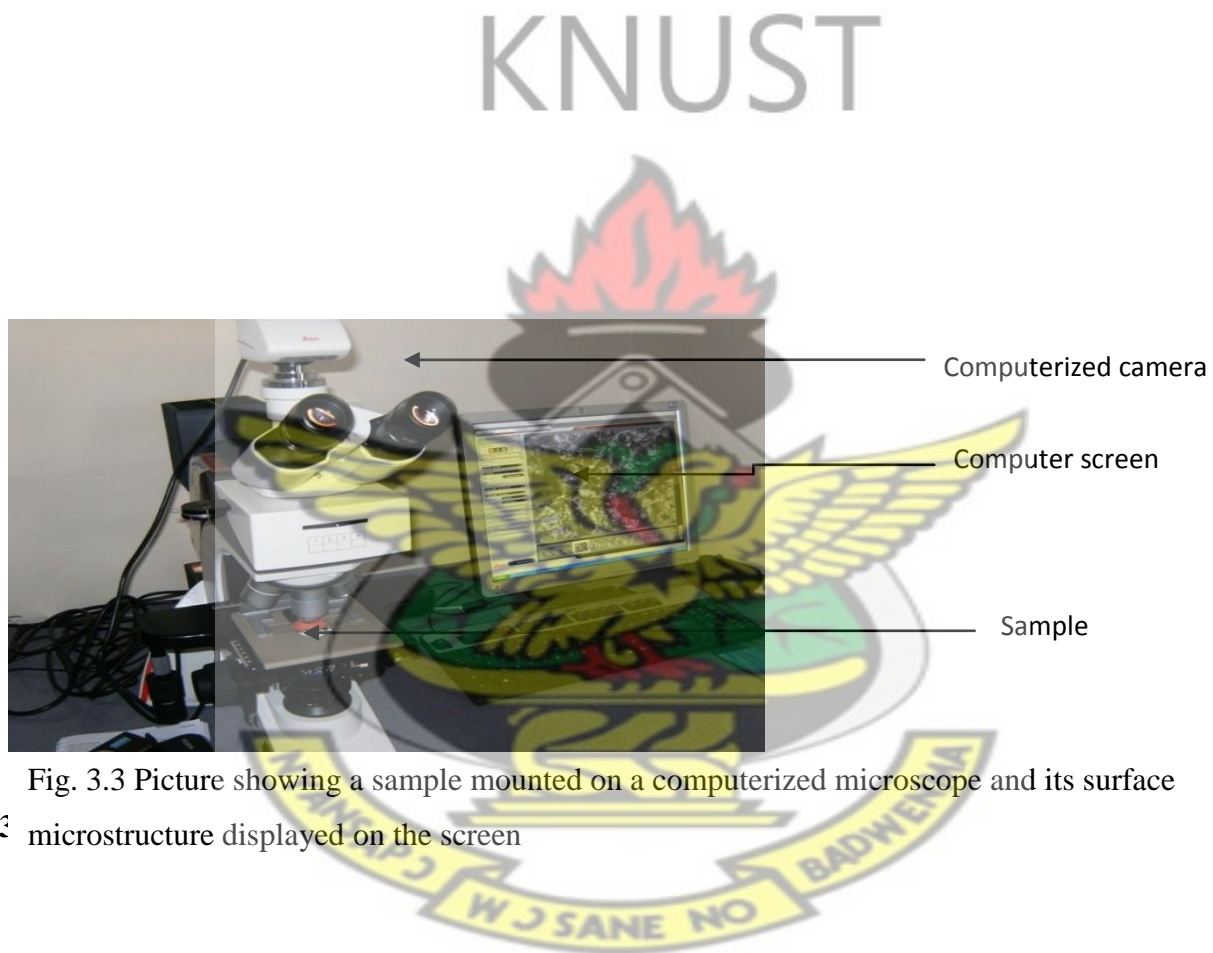

Fig. 3.3 Picture showing a sample mounted on a computerized microscope and its surface microstructure displayed on the screen

3.3.1 The Vickers Hardness Test

Each roofing sample was cut with shears into dimensions of 5cm x 5 cm, washed with soapy water and rinsed in hot water to remove stains such as oil from the surface. The sample was then fixed on a metal block of the same dimension using an adhesive to provide flat surface area for

the diamond indenter. The sample was positioned in the micro hardness tester for indenting the surface with the diamond indenter, in the form of a right pyramid with a square base and an angle of 136 degrees between opposite faces subjected to a load of 5kgf.

The full load was applied for 10 seconds. The two diagonals of the indentation left in the surface of the roofing sheet after removal of the load are measured using a microscope and their average calculated. The area of the sloping surface of the indentation was calculated and the Vickers hardness number calculated by substituting the two diameters (d_1 and d_2) measured into equation (3.4)
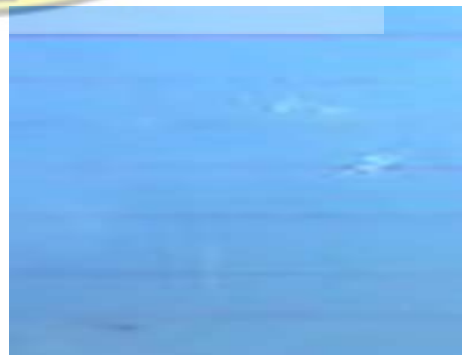
$$HV = \frac{2\,F\sin\frac{136}{2}}{d^2} \quad\text{...3.4}$$

$$HV = 1.854\frac{F}{d^2} \quad\text{...3.5}$$

Where

F = Load in kgf

and

d = Arithmetic mean of the two diagonals, d_1 and d_2 in mm

(a)   (b)

(c)   (d)

(e)

Figure 3.4 Prepared samples for micro hardness tests (a) G1*Jap (b) GC (c) AlZn3*
(d) G1*ind and (e) Al

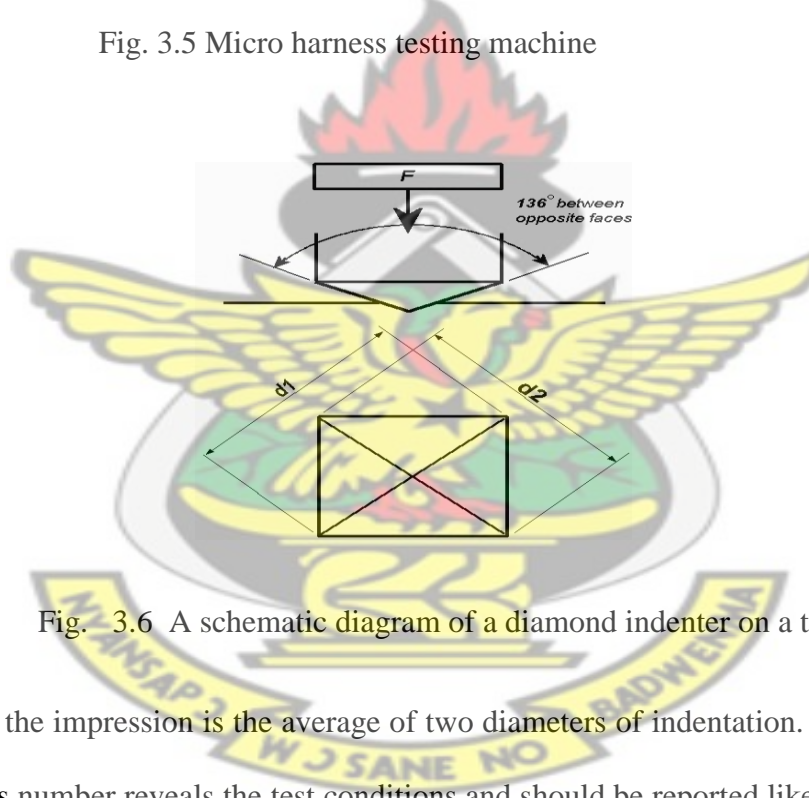Fig. 3.5 Micro harness testing machine

Fig. 3.6 A schematic diagram of a diamond indenter on a test specimen

The diameter of the impression is the average of two diameters of indentation. A well structured Vickers hardness number reveals the test conditions and should be reported like 800 HV/5 which means a Vickers hardness of 800, was obtained using a 5 kg force for 10 seconds. Several different loading settings give practically identical hardness numbers on uniform material, which is much better than the arbitrary changing of scale with the other hardness testing methods.

3.4   Tensile Tests

Sample sheets were cut with shears very slowly to avoid heating up of samples due to frictional force to the required shape and size as shown in the diagram below (Fig. 3.6). It was then cleaned thoroughly with soapy water and rinsed in warm water to remove clogged up dirt, grease and then sent to the Tinius Olsen super "L" hydraulic Universal Testing Machine (Model 602) control/display system (Fig.3.7) for tensile test to be done. The initial gauge length was measured.

The samples were positioned in the jaw of the tensile testing machine using the rack and pinion-type Flat Grips for testing flat specimens. The grip retainers were assembled at the top and lower crossheads placed in position and loosely fastened the screws holding the retainers. The pinion shaft handle was turned so that the gears engage the teeth on the wedge grips evenly. The handle was turned until the grips were fully inside the crosshead and the roofing sheets were inserted one after the other between the wedge grips, and the crank handle turned. The extensometer was connected to the sample.

 The function keys were used to set to zero the three displayed channels, i.e. the force, the position and auxiliary. The tensile machine was started to stretch the roofing sheet. At the breaking point the extensometer was removed from the sample and a graph of stress against strain was automatically plotted by the computer. The final gauge length was measured and value entered into the computer for the determination of the Young's Modulus of Elasticity, the Yield Stress, the 0.2 % offset, the Ultimate Tensile Stress, and the Breaking Stress and Energy.
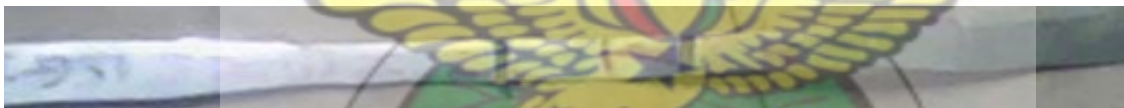

(a)

(b)

(c)

(d)

(e)

Fig. 3.7   Prepared samples for tensile tests (a) G1*Jap (b) GC (c) AlZn3* (d) G1*Ind and (e) AL
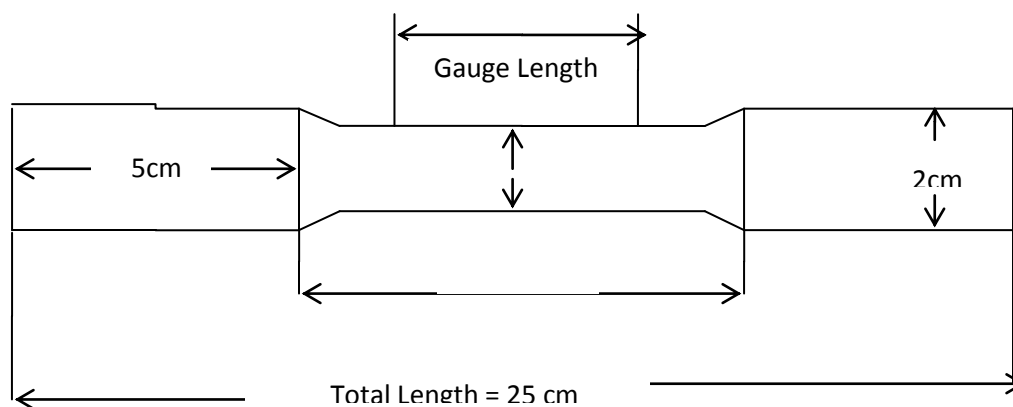
Figure 3.8 Schematic diagram of a prepared tensile test sample, (not drawn to scale)
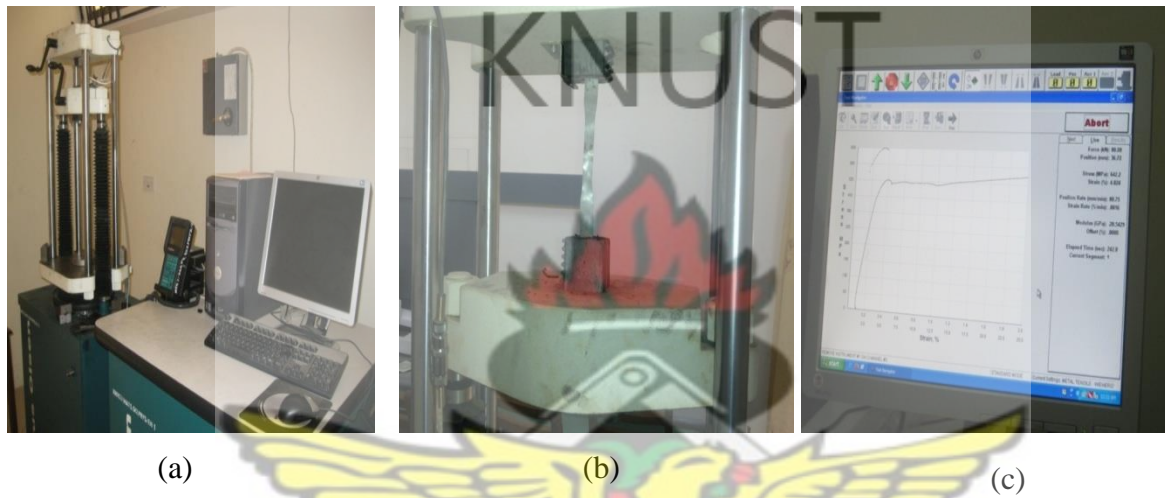
British Standard

(a)   (b)   (c)

Fig 3.9   Tensile testing machine (a), sample held in place (b) and monitor (c)

CHAPTER FOUR

RESULTS AND DISCUSSIONS

4.1 Tensile test

Figures 4.1– 4.5 below show the stress-strain curve of some metal roofing sheets. It provided information such as the Young's modulus, yield strength, ultimate tensile strength, ductility (measured in terms of percent elongation) as well as maximum breaking energy. The initial linear portion of the curves shows the proportional limit or elastic limit. This showed that Hooke's law is obeyed, as the strain material being proportional to applied stress, within the elastic limit. This is due to the inter-atomic interaction of carbon atoms and dislocations in the stressed metal roofing sheet. The various phases present in the microstructure give reason for such mechanical behavior. For this reason, the roofing sheet suffers plastic deformation before it fractures, by slow crack propagation. After thinning uniformly along its length during the plastic stage, the metal sheet developed a minimal 'waist' or 'neck' which form cavities. Possibility of internal cavities formation during the later stages of the plastic strain when stress concentration arise in regions having a large number of interlocking dislocations.
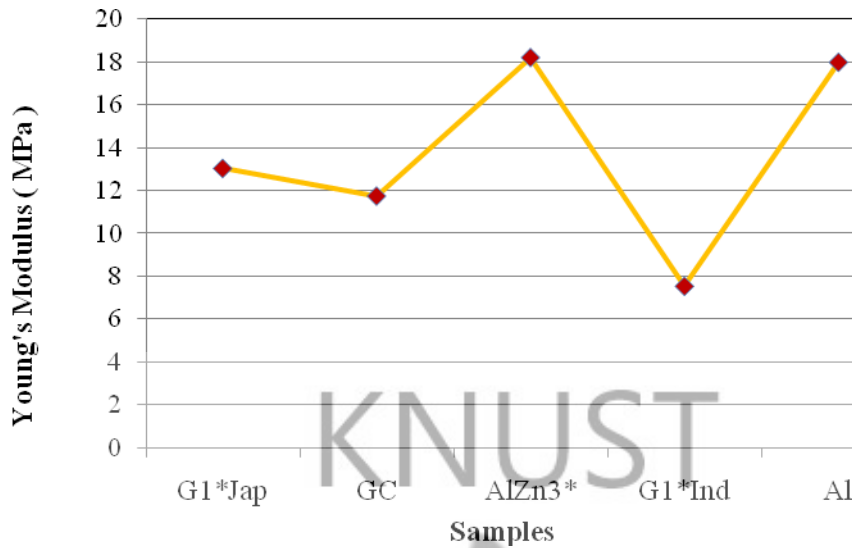
Fig. 4.1 Young's Modulus of Elasticity for various roofing sheets

From Fig. 4.1 it can be seen that the average Young's Moduli of Elasticity for different samples (One star galvanized sheet Japan [G1*Jap], Galvanized coated (GC), Aluzinc three star galvanized [AlZn3*], One star galvanized India [G1*Ind] and Aluminum [Al] sheets) were 13.05 ± 1.33 MPa, 11.76 ± 2.61 MPa, 18.21 ± 1.42 MPa, 7.57 ± 1.56 MPa and 17.99 ± 5.89 MPa respectively (Table 4.1 show details of calculated values). Fig 4.1 shows that AlZn3* had the highest Young's modulus of elasticity value than Al whiles G1*Ind had the least. This is an indication that AlZn3* developed a greater ability to recover under a given load or stress compared to the Al, G1*Jap and G1*Ind. The internal stress and increase of mobile dislocations density explained why AlZn3* was harder and more brittle than the Al and other roofing sheets. Hence the higher Young's Modulus value which accounted for AlZn3*able to bear a highest load than the Al and other roofing sheets.
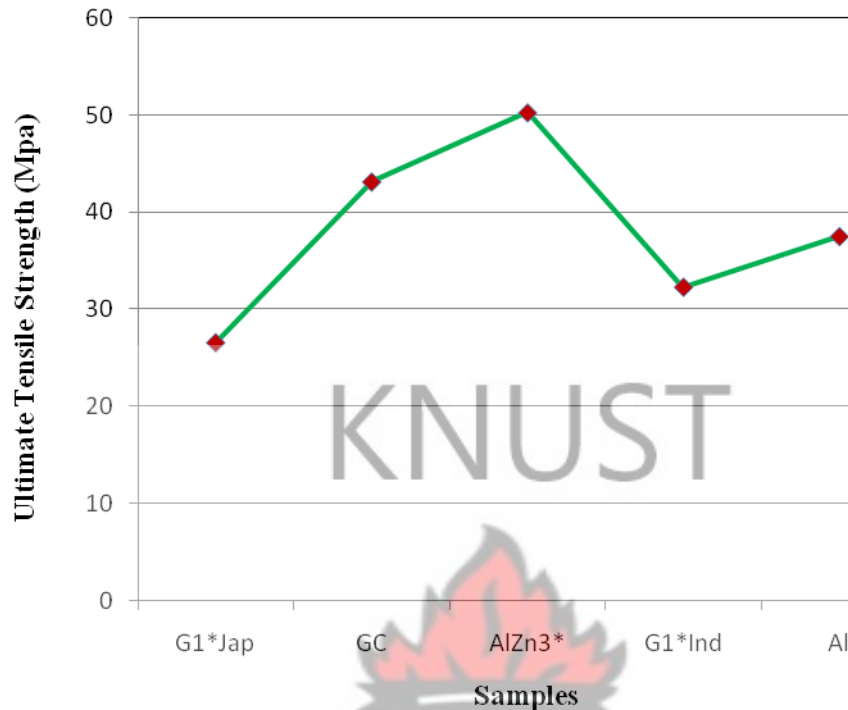
Fig. 4.2 Average Ultimate Tensile Strength for different roofing sheets

The Yield points of the roofing sheets were indication of the Toughness or Ultimate Tensile Strength. From Fig. 4.2 the average Ultimate Tensile Strength for G1*Jap, GC, AlZn3*, G1*Ind Al sheets were 26.59 ± 1.57 MPa, 43.25 ± 6.97 MPa, 50.27 ± 2.57 MPa, 32.31 ± 2.52 MPa, and 37.52 ± 3.99 MPa respectively. AlZn3* showed relatively good strength and toughness with an average value of 50.27 ± 2.57 MPa and GC had an average value of 43.25 ± 6.97 MPa with G1*Jap showing the least average value of 26.59 ± 1.57 MPa. AlZn3* can best be described as being exceptionally strong, evident from the higher elastic limit and also could bear more load before fracture than other roofing sheets. This property makes AlZn3* ideal for installation due to load exerted on it by workers.
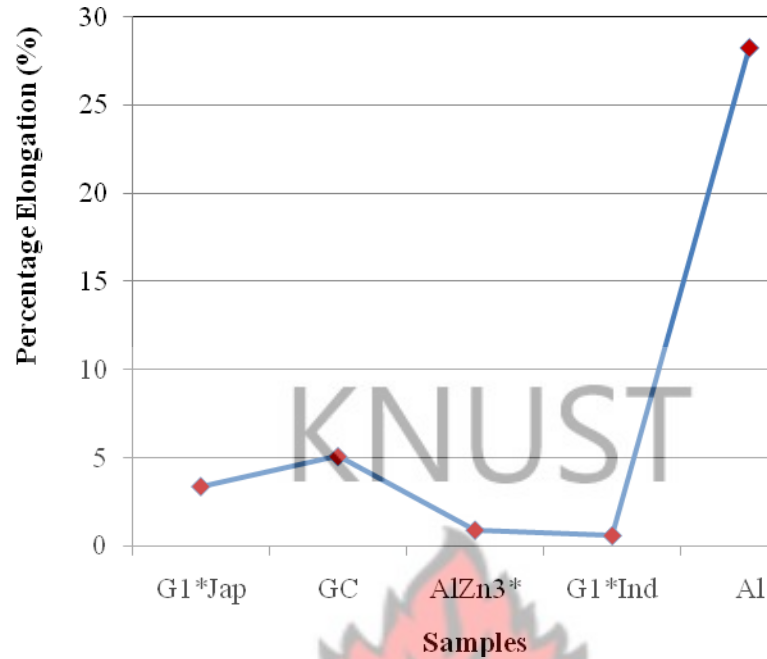
Fig. 4.3 Percentage Elongation of various roofing sheets

It can be deduced from Fig. 4.3 that the average Young's Modulus of elasticity for different roofing sheets G1*Jap, GC, AlZn3*, G1*Ind and Al sheets were 13.05 ± 0.18 %, 11.76 ± 4.16 %, 18.21 ± 0.15 %, 7.57 ± 0.05 % and 17.99 ± 0.77 % respectively. ALZn3* had the highest Young's modulus of elasticity value than Al whiles G1*Ind had the least value. This is an indication that AlZn3* developed a greater ability to recover under a given load or stress as compared with Al, G1*Ind, G1*Jap and GC roofing sheets.
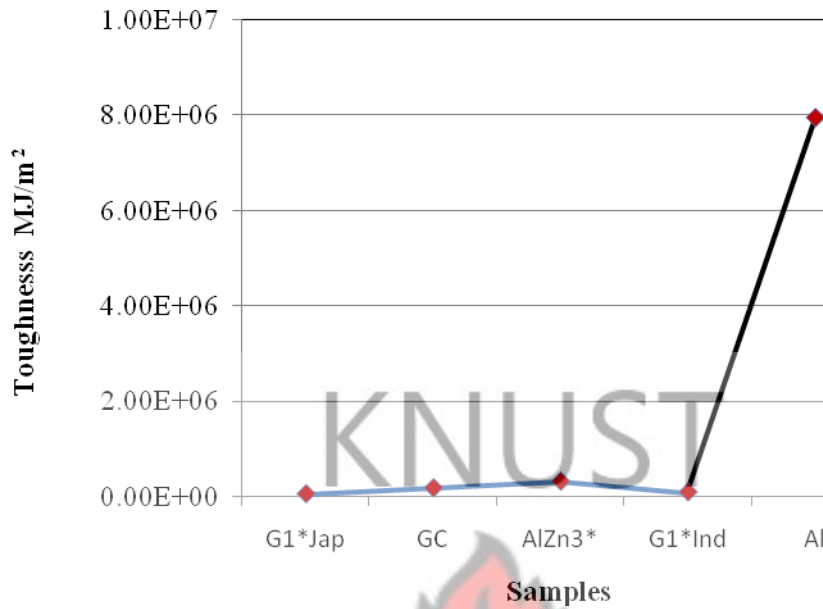
Fig. 4.4 Maximum Breaking energy for various roofing sheets

From Fig. 4.3 it can be seen that the average Breaking Energy for different samples G1*Jap, GC, AlZn3*, G1*Ind and Al roofing sheets were 55378 ± 22666 MJm^{-2}, 177770 ± 41956.3 MJm^{-2}, 316810 ± 74578.7 MJm^{-2}, 92230 ± 14285.0 MJm^{-2} and 7956600 ± 48769.02 MJm^{-2} respectively. It indicated that Al showed a higher with a value whiles G1*Ind and G1*Jap showed very close breaking energy values of 55378 ± 22666 and 92230 ± 14285.0MJm^{-2}. This was an indication that Al could bear more loads before fracture than the other roofing sheets. With an increase in load beyond the Yield point Al slowly stretched to a point where the cross-sectional area supports no additional load. The maximum stress, provided information on the high stress the roofing sheet could withstand, i.e. the maximum load the sheet could bear before fracture. G1*Jap, GC, AlZn3* yielded quickly to reach their maximum stress as indicated in Fig.4.3 but gave shorter total extension before fracture. G1*Jap, GC, AlZn3* were hard and brittle as a results of the thermo metallurgical treatment (TMT). Aluminum [Al] roofing sheet stretched

more than other roofing sheets under less applied load. This is obvious from the stress-strain curves in Fig.4.3 as the stress decreased gradually to the point where the roofing sheet fractured.

Fig. 4.5 Comparing the average Ultimate Tensile Strength and Percentage Elongation of different roofing samples

Fig. 4.5 shows that a metal with a high Ultimate Tensile Strength does not necessarily have a good ductility or a good plastic deformation. AlZn3* could bear more loads but could not extend more than Al before fracturing. It is an indication that Al roofing sheet were more ductile than AlZn3*.
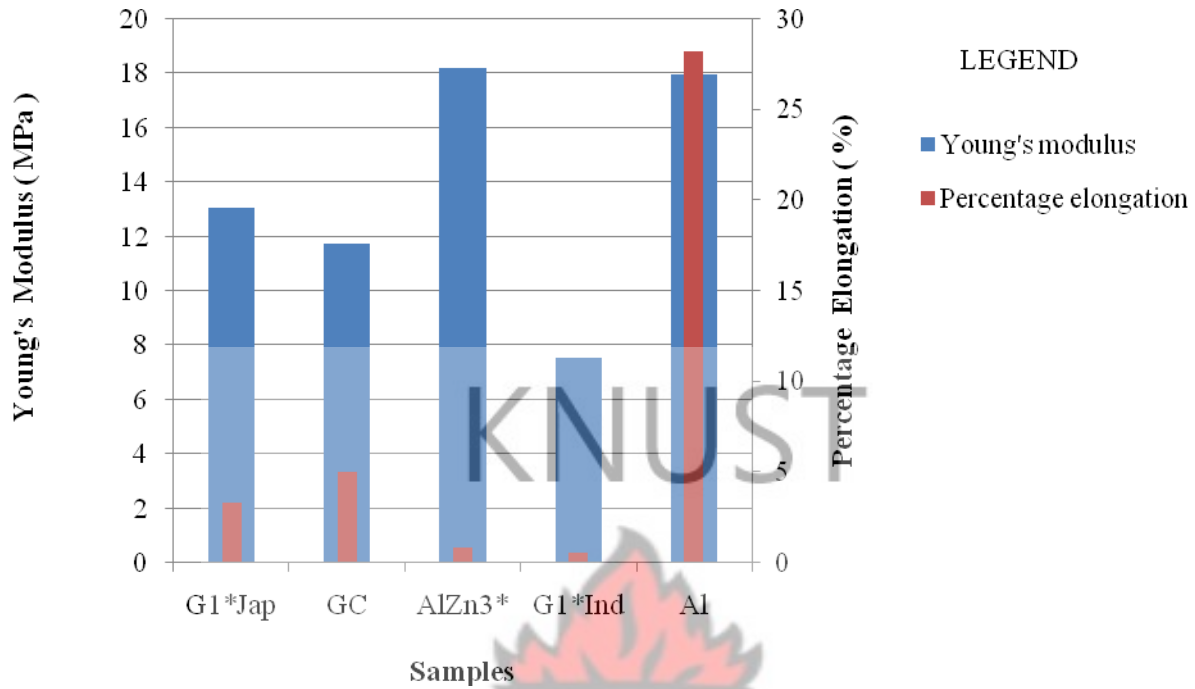
g. 4.6 Comparing the average Young's Modulus and Percentage Elongation of different roofing sheets.

Fig. 4.6 shows that AlZn3* sheets could bear more loads before fracture as compare with Al roofing sheets. Young's Modulus which is stress divided by strain just showed the resistance of the atoms in the structure to plastic deformation. From the hardness test results shown in Table.4.1 AlZn3* had the highest average hardness value of 3875.4 ± 947.0 Nm^{-2} followed by G1*Jap with value 797.0 ± 365 Nm^{-2} and Al having the least value of 67.3 ± 12.99 Nm^{-2}. This indicated that AlZn3* sheet was hardest since it lack lacks of plasticity while Al sheet was ductile as it could absorb more energy before fracture and this is manifested by the high value the Percentage Elongation.
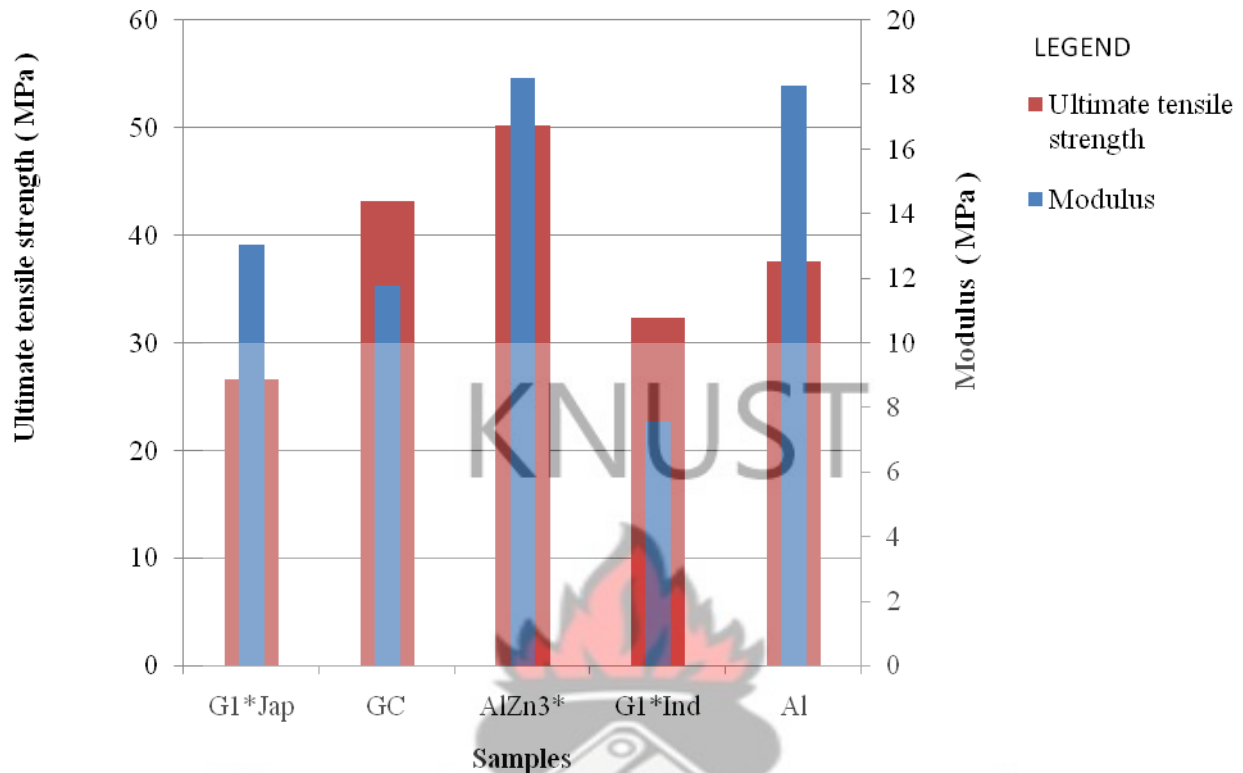
Fig. 4.7 Comparing the average Ultimate Tensile Strength and Toughness of different roofing
sheets

Fig.4.7 shows that if a metal sheet is tough it does not necessary have a high Ultimate Tensile
strength. A material may not be tough but can bear a lot of load before fracture. Since toughness
means the ability of a material to absorb energy and not the amount of load it can bear. Al sheet
was more ductile than AlZn3* whiles G1*Ind sheet showed a lower ductility. AlZn3* sheet
showed a high Ultimate Tensile Strength and also Modulus of Elasticity.

4.2 Micro – Hardness Tests

Table 4.1   Average Micro Hardness for all samples

Sample Identity	Micro Hardness / Nm^{-2}
G1*Jap	797 ± 366
GC	377 ± 101
AlZn3*	3875 ± 947
G1*Ind	195 ± 48
Al	67 ± 13

From the hardness test results (in Table. 4.2) G1*Jap, GC, AlZn3*, G1*Ind and Al had an average hardness value of 797 ± 365Nm^{-2}, 377 ± 10 Nm^{-2}, 3875 ± 947 Nm^{-2}, 196 ± 48 Nm^{-2} and 67 ± 13 respectively. AlZn3* had the highest value followed by G1*Jap with Al having the least value since it is more ductile and can withstand both plastic and elastic deformations. It is an indication that AlZn3* with higher Yield Strength had a higher hardness (more brittle) and also the hardness of AlZn3* with strong strain-hardening ability is not only affected by the fracture strength but also by the Yield Strength. Thus, the ability of the AlZn3* resisting permanent deformation is relatively stronger, resulting in a higher hardness. This might be one of reasons why the hardness of AlZn3* increases with increasing the atomic bonding properties of different composites in the materials. The Percentage Elongation and the reduction in area in tension are often used as empirical measures of ductility. The atomic bonding property increases with increasing the atomic bonding and this accounted for the ductile nature of Aluminum.

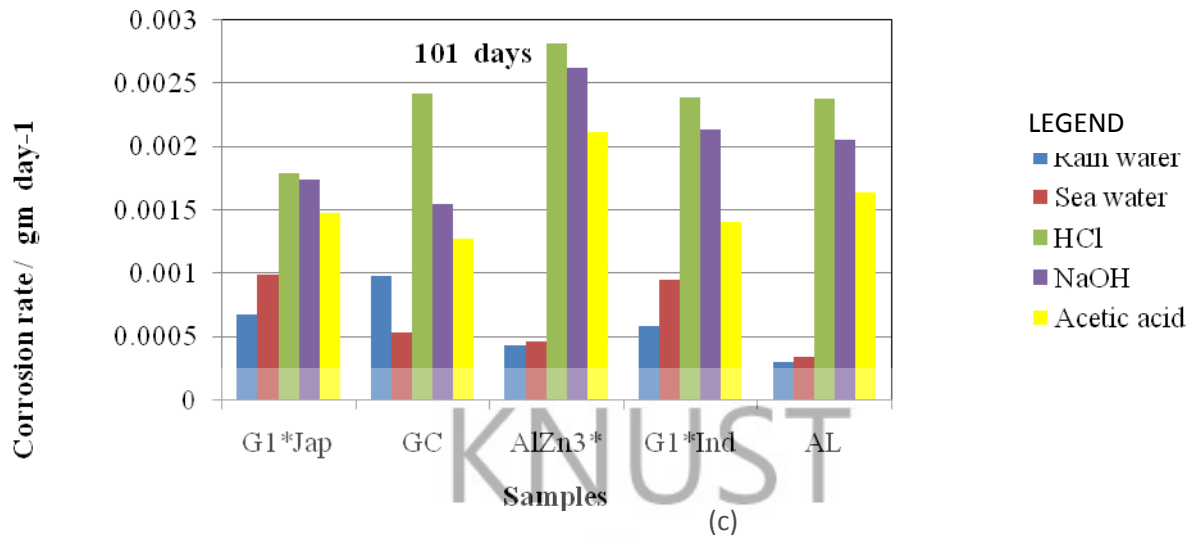## 4.3 Corrosion Tests
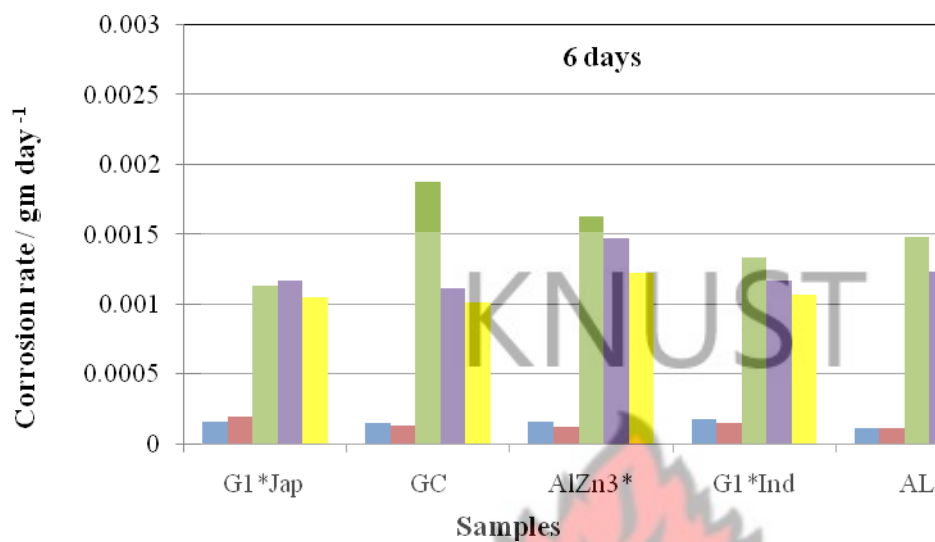
(a)
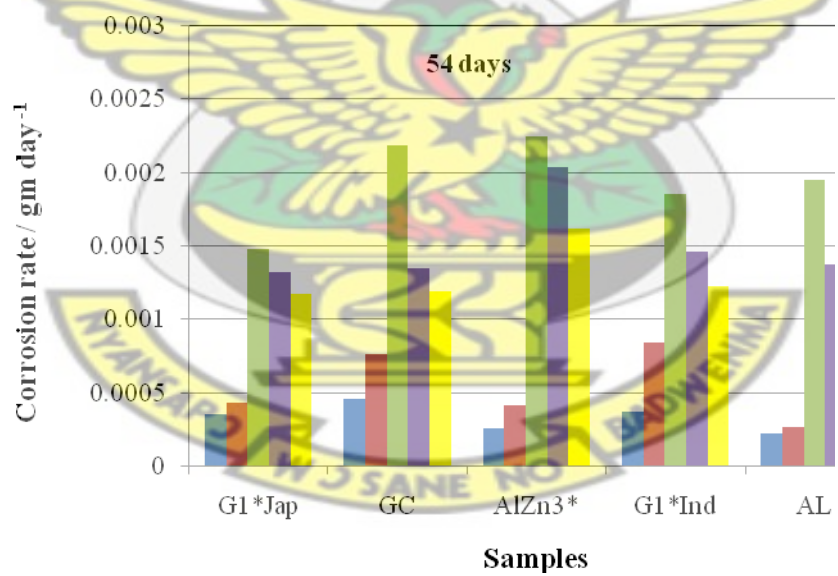
(b)

Fig. 4.8 Comparing corrosion per day of different solutions on each sample for some selected number of days (a) 6 days (b) 54 days and (c) 101 days
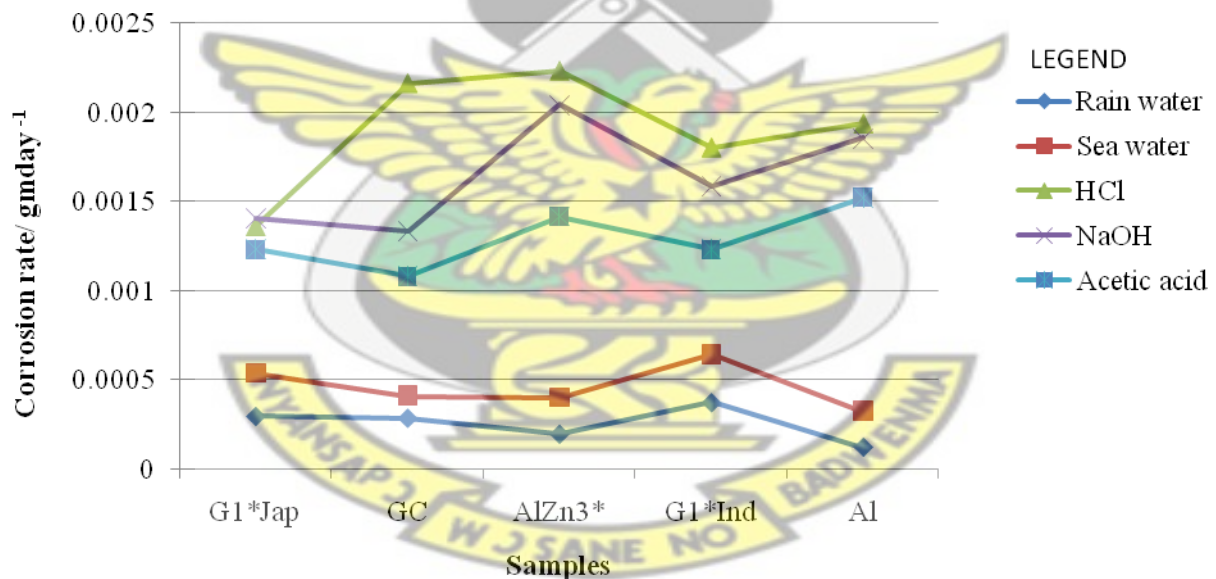

Fig. 4.9 Average corrosion rate per day of different solutions on each sample for the entire period of

101

Fig. 4.8 (a) shows that corrosion per day increased for each sample immersed in different solutions for 6 days. Within 6 days period, corrosion per day for 0.5M hydrochloric acid was highest on AlZn3* (0.001633 gm/ day), followed by GC (0.001877 gm/ day) with G1*Jap (0.001133 gm/ day) being the least corroded. Over the same period, corrosion per day of 0.2 M sodium hydroxide solution was higher on AlZn3* (0.001476 gm/ day) whiles GC (0.00116 gm/ day) was least corroded. Corrosion rate of 0.5 M acetic acid was highest on Al (0.001345 gm/day) AlZn3* (0.001224 gm/ day) being next and G1*Jap (0.000547 gm/ day) with the least value. Al was least affected by both rain sea water (0.000111 gm/ day, 0.0001164 gm/day since it has the ability to form oxide on its surface when scratch forms on its surface. G1*Jap (0.0001933 gm/ day) was highly affected by sea water while G1*Ind (0.0001767 gm/ day) had the highest corrosion per day in rain water rain and sea water.

 From Fig. 4.8 (b) shows that corrosion per day increased for each sample immersed in different solutions for 54 days was highest for 0.2 M hydrochloric acid solution followed by 0.5 M sodium hydroxide with rain water having the least value. Within 54 day period corrosion per day for 0.5 M hydrochloric acid was highest on AlZn3*(0.001855 gm/ day) followed by Al (0.001953 gm/ day) with GC (0.002189 gm/day) having the minimum value. Over the same period, the corrosion per day of 0.5 M sodium hydroxide solution was highest on G1*Ind (0.001459gm/day) followed by Al (0.001593 gm/day) with AlZn3* (0.002935gm/day) having the least value.. The 0.2 M acetic acid solution effectively corroded AlZn3* (0.001621 gm/day) with G1*Jap (0.00029757 gm/day) having the minimum value. Al was least affected by both rain and sea water (0.0002255 gm/day, 0.0003422 gm/day since it has the ability to form oxide on its surface when scratch forms on its surface. G1*Jap (0.0001933 gm/ day) was highly affected by sea water

while G1*Ind (0.0001767 gm/ day) had the highest corrosion per day in rain water rain and sea water.

The bar charts in fig 4.8 (c) show the effect of different solutions on each roofing sample for 90 days. Effect of 0.5 M hydrochloric acid was highest on AlZn3* (0.002812 gm/ day) followed by GC (0.002419 gm/day) G1*Jap (0.001783) having the minimum value.

Over the same period, corrosion per day for 0.5 M sodium hydroxide solution was highest on AlZn3*(0.002619 gm/day) whiles GC (0.00154 gm/day) with the least corrosion rate value. Corrosion rate of 0.5 M acetic acid solution highest on Al (0.001632 gm/day) followed by G1*Ind (0.001403 gm/day) with G1*Jap (0.000692 gm/day) being the least. Corrosion rate per day of sea water was highest on G1*Jap (0.0006704 gm/day) ; followed by G1*Jap (0.0006704 gm/day) and Al (0.0002976 gm/day) showing the least value .

In rainwater, GC showed highest rate of corrosion of 0.0009763 gm/ day and AlZn3* recorded the minimum corrosion rate value of 0.000006311 gm/ day.

As observed from Fig. 4.8 (a) – (b) the average corrosion per day for solutions with high acidity increased over the   whole period of the experiment and it is an indication of the accelerated behavior of the metal dissolution. This result is expected because with acidic content of hydrochloric acid solution, both H^+ ion and Cl- ion concentrations increased.
 Iron dissolution in hydrochloric acid solutions depends principally upon H+ ion more than the Cl⁻ ion.

 The hydrogen gas evolution and mass loss is produced is shown in equation 4.1

$$Fe \text{ (solid)} + 2 H^+ = Fe^{2+} + H_2 \text{ (gas)} \quad \dots\dots\dots\dots\dots\dots\dots\dots\dots 4.1$$
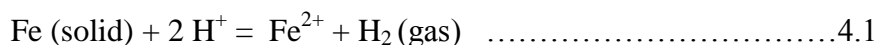
Surface micro structural studies for each roofing sample was performed before and after immersing the samples in the various solutions for 6, 54 and 90 days as illustrated in

Figures 4.10 – 4.34 below. Considering the micrographs for each sample immersed in 0.2 M hydrochloric acid solution revealed that the corrosion attack (general and pitting corrosion) becomes more pronounced in hydrochloric acid solution and these pits were full of black corrosion products. These observations can be explained on the basis of Cl^- ion activity and the extent of its contribution in accelerated metal dissolution. Since corrosion rate per day is greatly affected by the presence of H^+ ion , the absence of H^+ ion in sodium hydroxide, acetic acid (being a base and weak acid), rain water and sea water. This accounted for their low corrosive rates on different roofing samples.
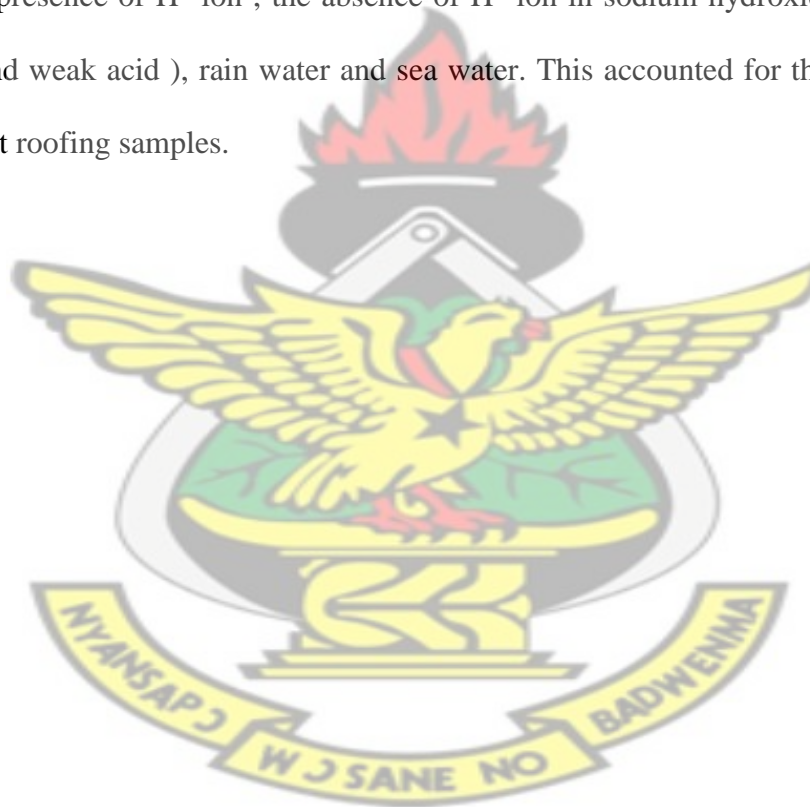
Surface Micrographs of different Samples Immersed in Different Solutions

G1*Jap   GC   AlZn3*   G1*Ind   Al
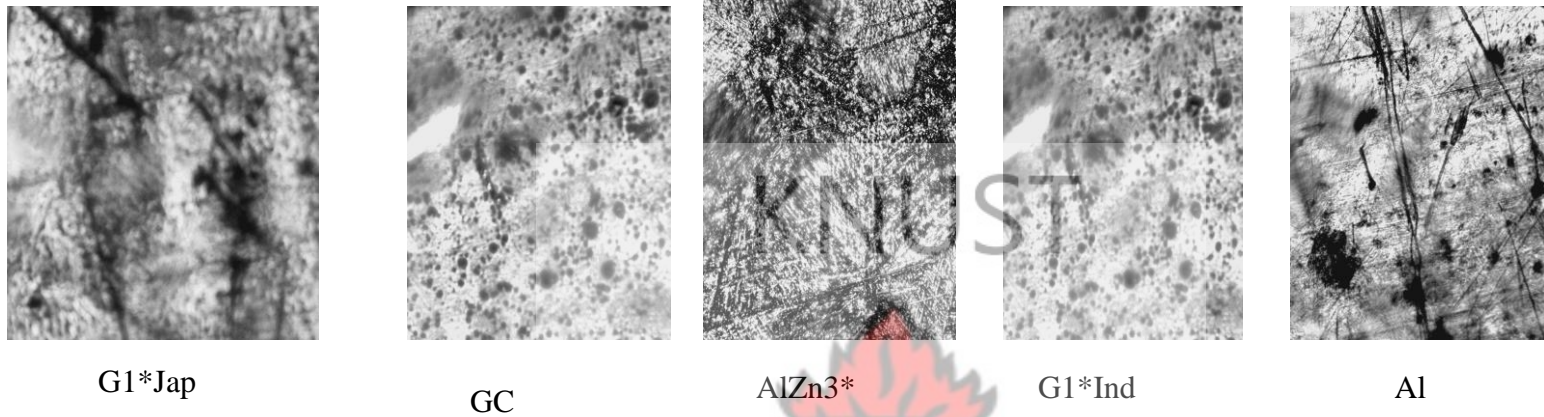
4.10 Microstructures obtained from different samples before experiment
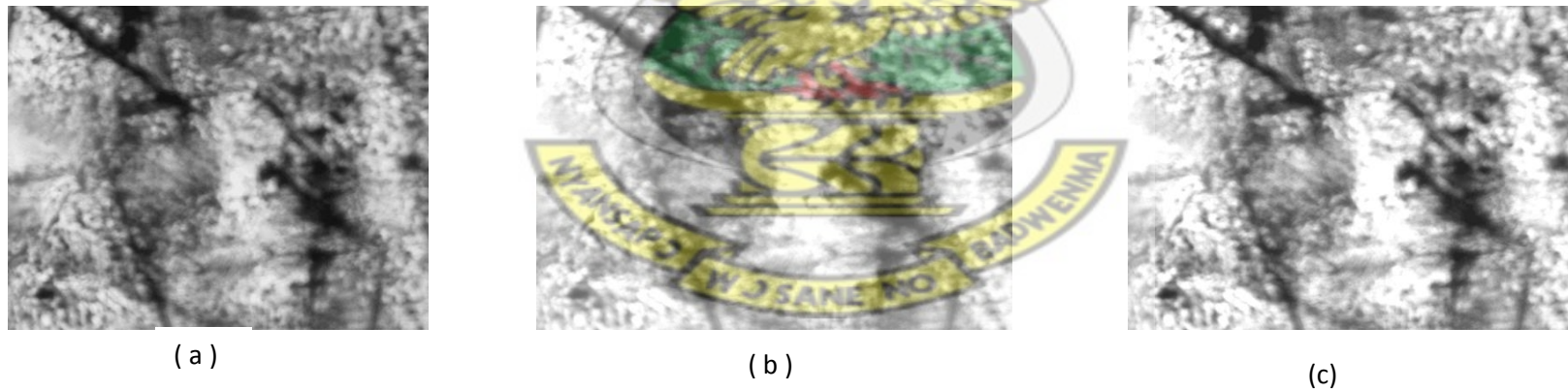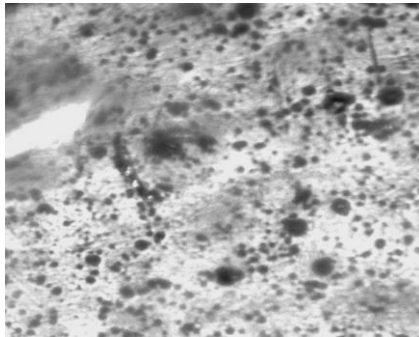

(a)   (b)   (c)

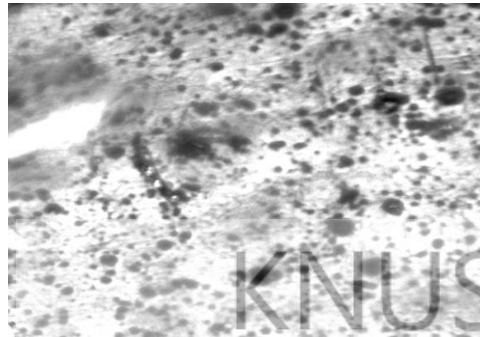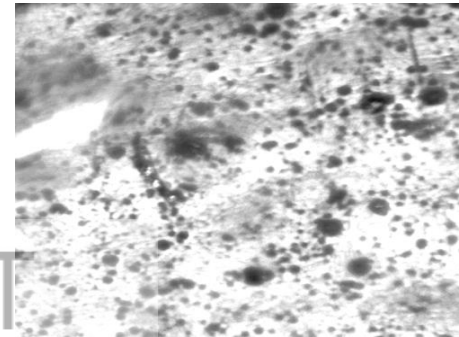Fig 4.11 Microstructures of G1*Jap roofing sheets immersed in 0.2 M HCl for (a) 6 days (b) 54 days and (c) 90 days

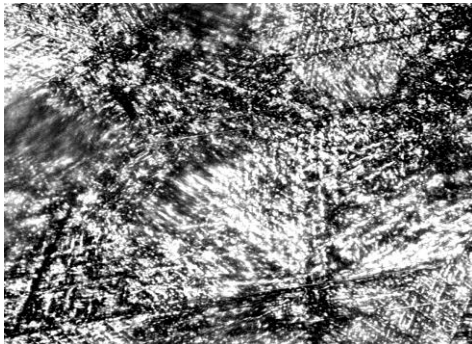(a)   (b)   (c)
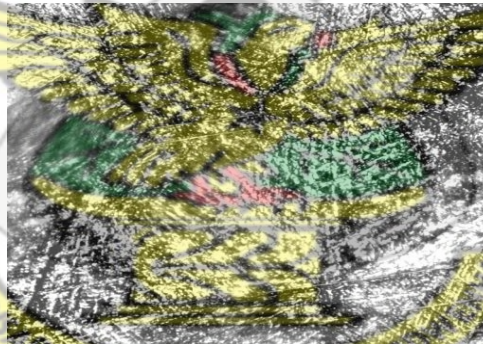
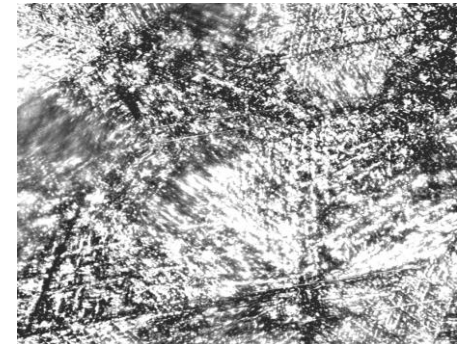Fig 4.12 Microstructures of GC sheets immersed in 0.2 M HCl for (a) 6 days (b) 54 days and (c) 90 days

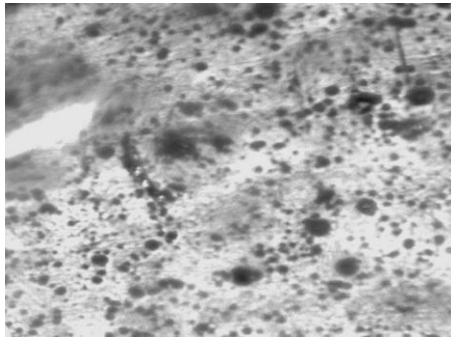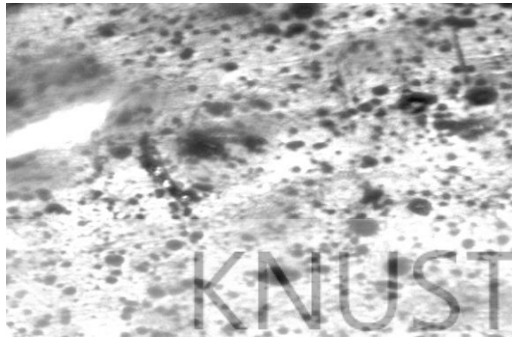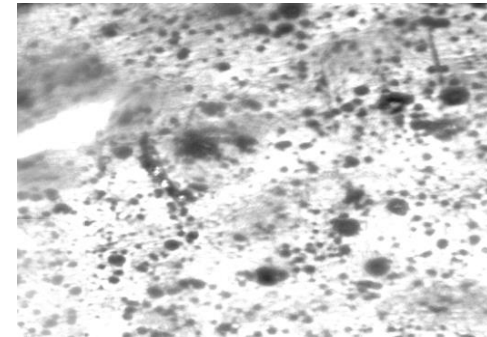(a)   (b)   (c)

Fig 4.13 Microstructures of AlZn3* sheets immersed in 0.2 M HCl for (a) 6 days (b) 54 days and (c) 90 days

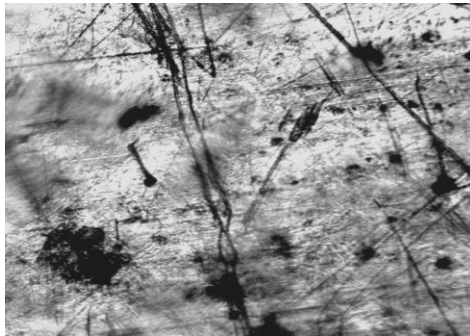(a)   (b)   (c)

Fig 4.14 Microstructures of G1*Ind sheets immersed in 0.2 M HCl for (a) 6 days (b) 54 days and (c) 90 days

(a)   (b)   (c)

Fig 4.15 Microstructures of Al sheets immersed in 0.2 M HCl for (a) 6 days (b) 54 days and (c) 90 days

<div align="center">(a)   (b)   (c)</div>

Fig 4.16 Microstructures of G1*Jap roofing sheets immersed in 0.5 M NaOH for (a) 6 days (b) 54 days and (c) 90 days

<div align="center">(a)   (b)   (c)</div>

Fig 4.17Microstructures of GC sheets immersed in NaOH solution for (a) 6 days (b) 54 days and (c) 90 days

(a)   (b)   (c)

Fig 4.18 Microstructures of AlZn3* sheets immersed in NaOH for (a) 6 days (b) 54 days and (c) 90 days
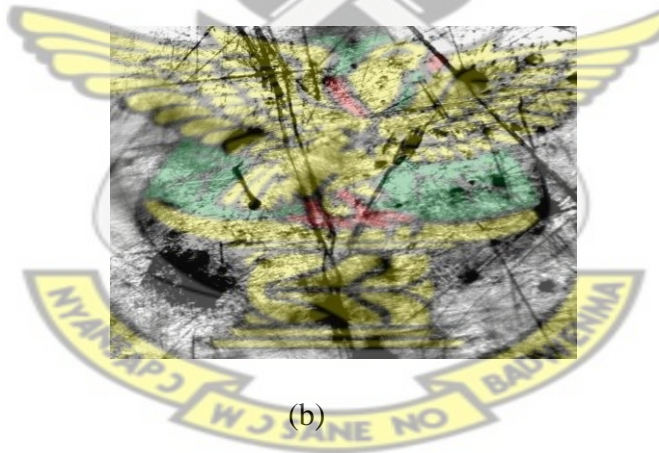
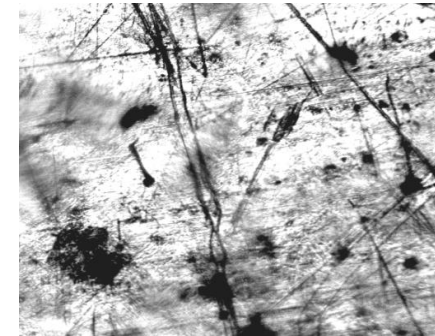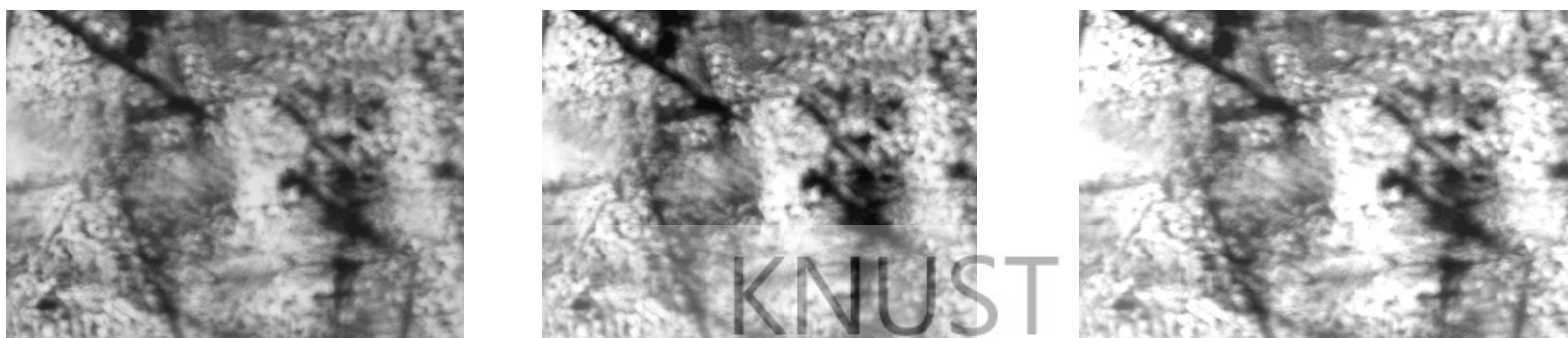

(a)   (b)   (c)

Fig 4.19 Microstructures of G1*Ind sheets immersed in NaOH for (a) 6 days (b) 54 days and (c) 90 days

(a)	(b)	(c)

Fig 4.20 Microstructures of Al sheets immersed in NaOH solution for (a) 6 days (b) 54 days and (c) 90 days
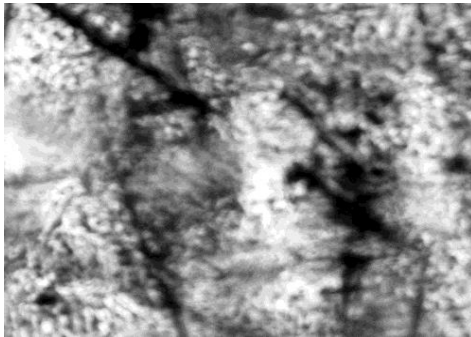
(a)	(b)	(c)

Fig 4.21 Microstructures of G1*Jap immersed in acetic acid solution for (a) 6 days (b) 54 days and (c) 90 days
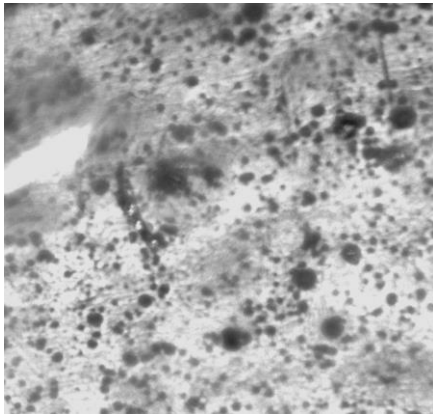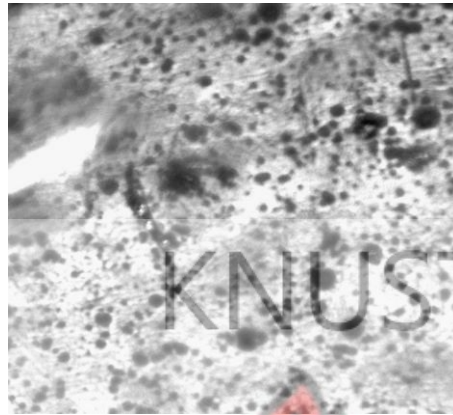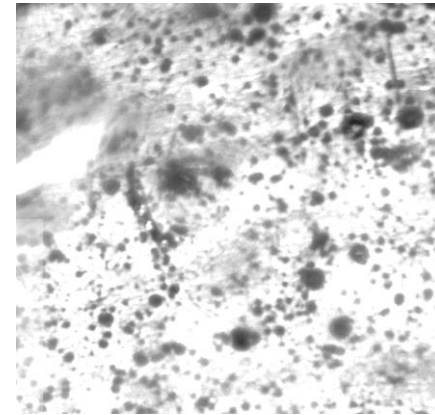
(a)	(b)	(c)

Fig 4.22 Microstructures of GC sheets immersed in acetic acid solution for (a) 6 days (b) 54 days and (c) 90 days

(a)	(b)	(c)

Fig 4.23 Microstructures of AlZn3* immersed in acetic acid solution for (a) 6 days (b) 54 days and (c) 90 days

(a)   (b)   (c)

Fig 4.24 Microstructures of G1*Ind immersed in acetic acid solution for (a) 6 days (b) 54 days and (c) 90 days
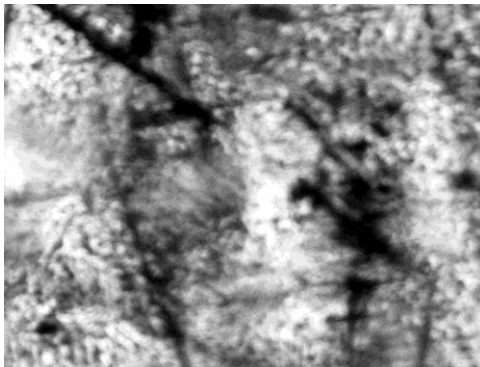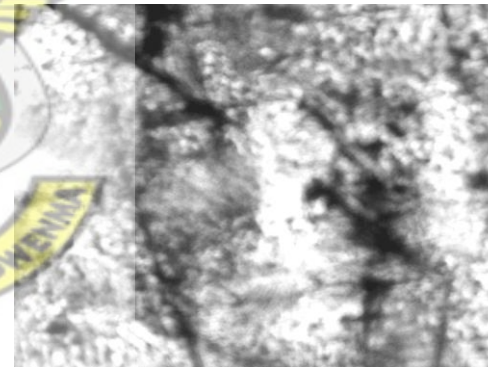
(a)   (b)   (c)

Fig 4.25 Microstructures of G1*Jap sheets immersed in rain water for (a) 6 days (b) 54 days and (c) 90 days
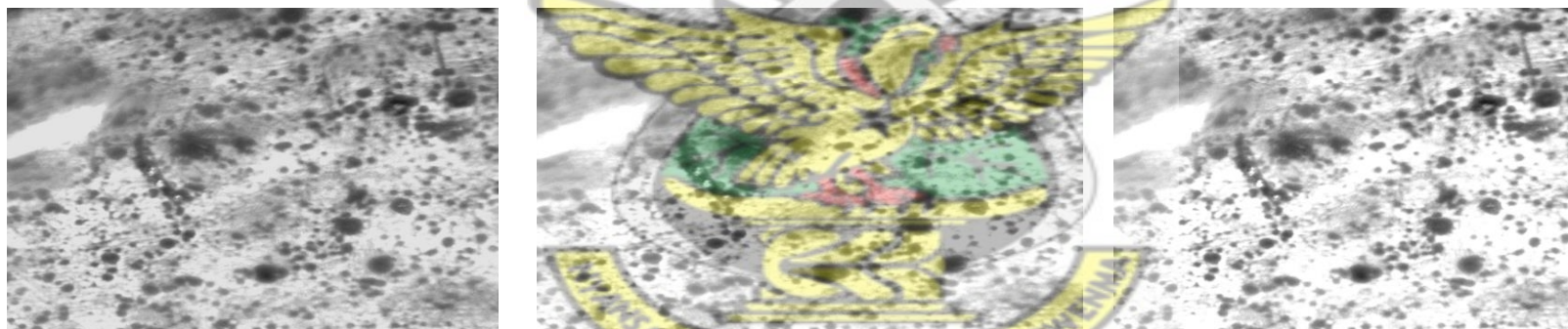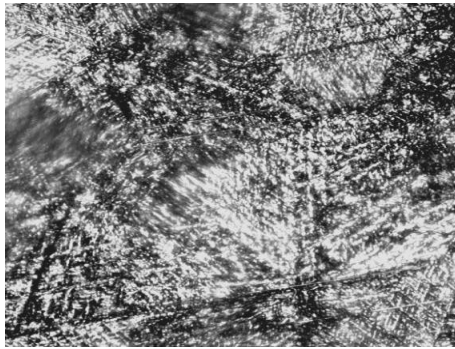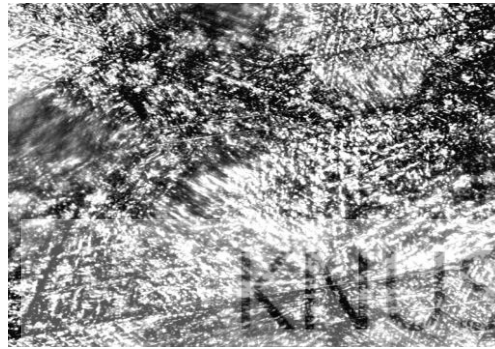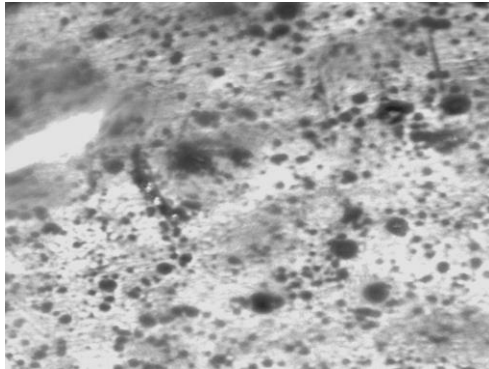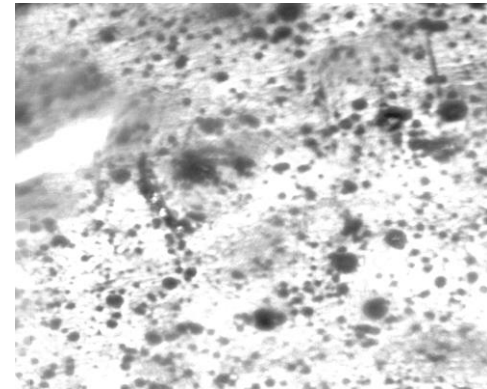
(a)   (b)   (c)

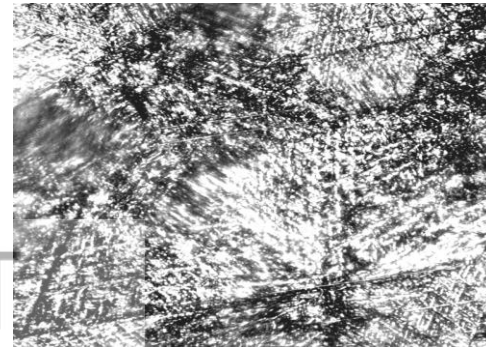Fig 4.26 Microstructures of GC sheets immersed in rain water for (a) 6 days (b) 54 days and (c) 90 days
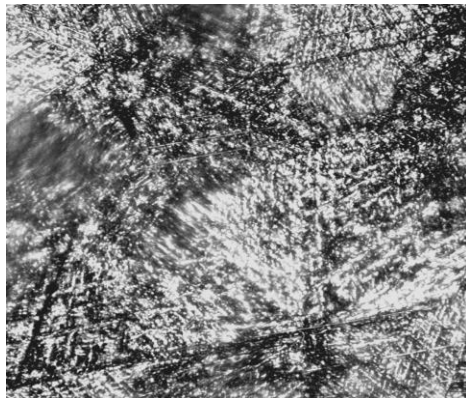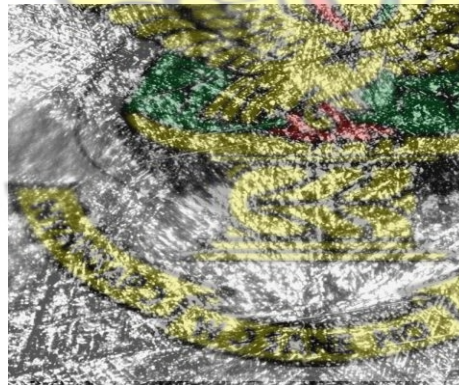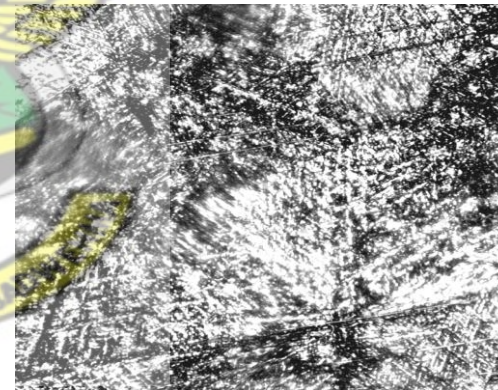
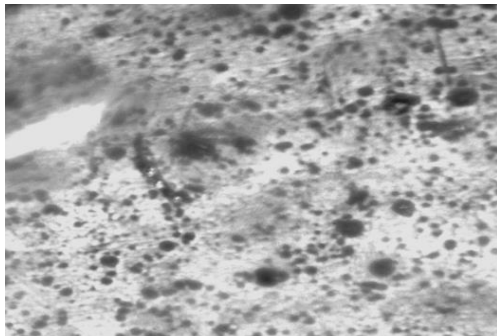(a)   (b)   (c)
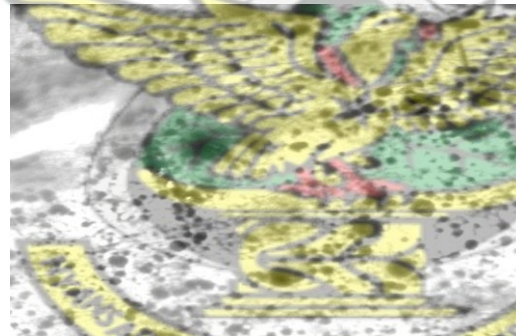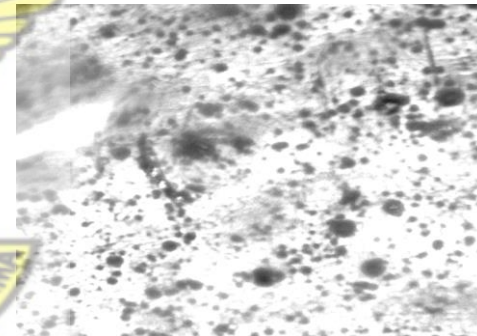
Fig 4.27 Microstructures of AlZn3* sheets immersed in rain water for (a) 6 days (b) 54 days and (c) 90 days
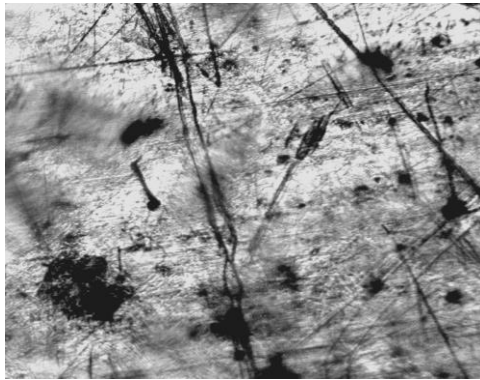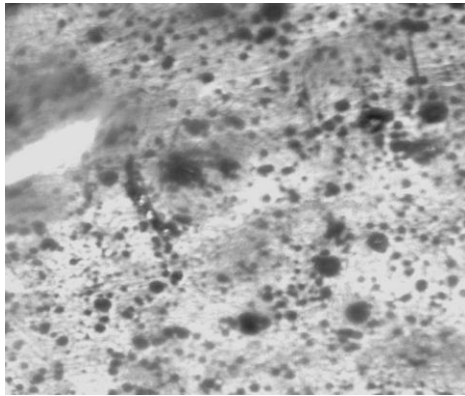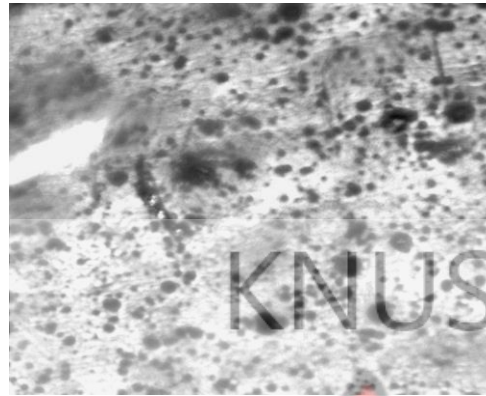
(a)   (b)   (c)
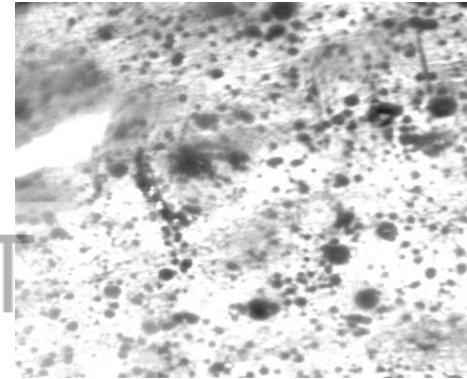
Fig 4.26 Microstructures of G1*Ind sheets immersed in rain water for (a) 6 days (b) 54 days and (c) 90 days
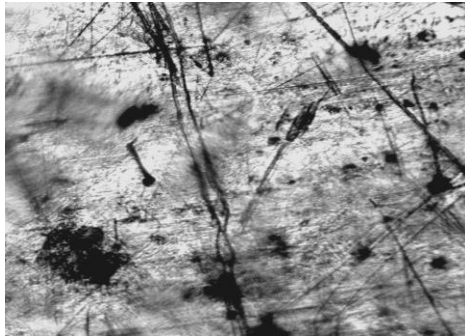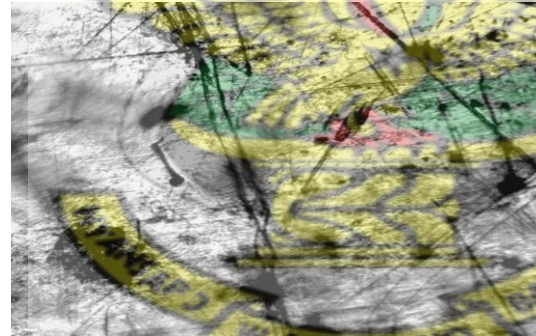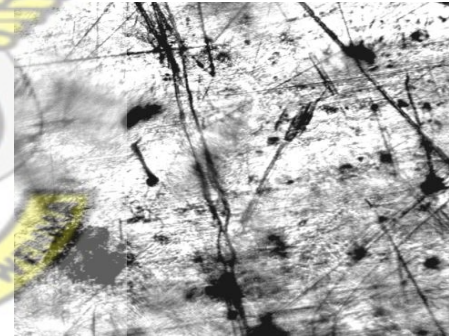
(a)   (b)   (c)

Fig 4.29 Microstructures of Al sheets immersed in rain water for (a) 6 days (b) 54 days and (c) 90 days
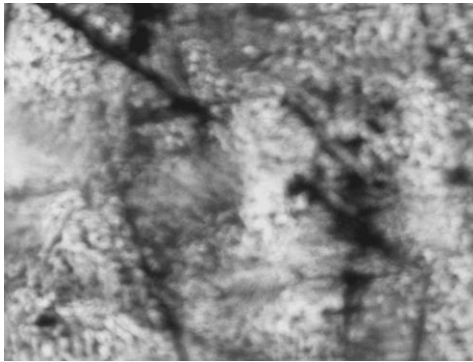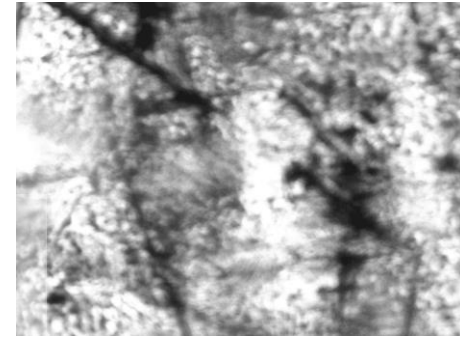
| (a) | (b) | (c) |

Fig 4.30 Microstructures of G1*Jap sheets immersed sea water for (a) 6 days (b) 54 days and (c) 90 days
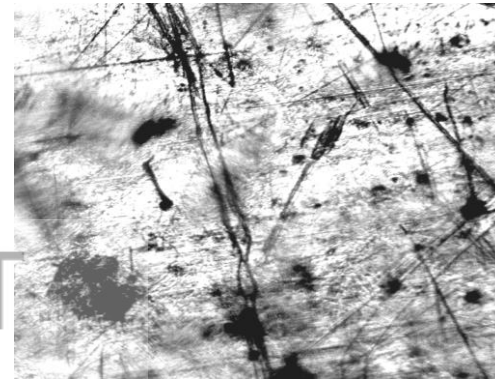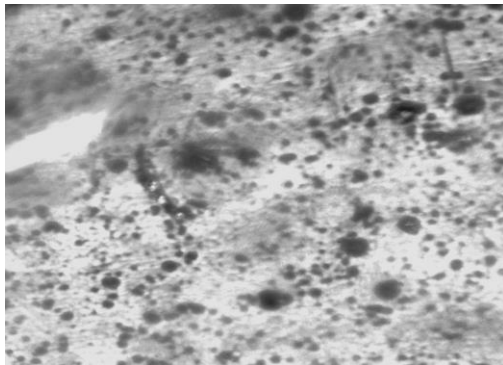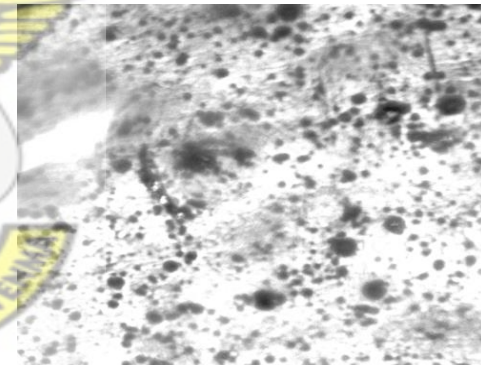

| (a) | (b) | (c) |

Fig 4.31 Microstructures of GC sheets immersed in sea water for (a) 6 days (b) 54 days and (c) 90 days
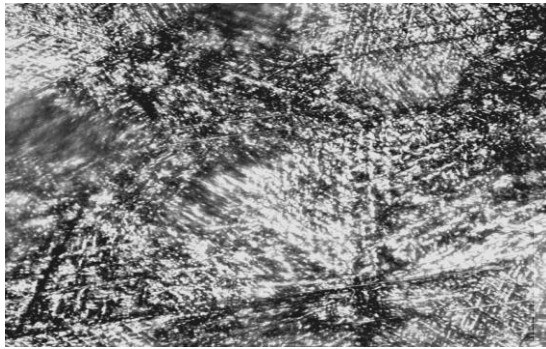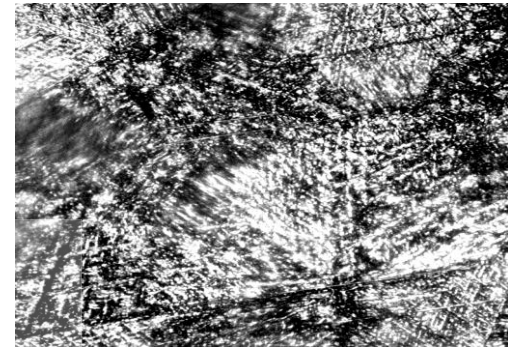
(a)   (b)   (c)

Fig 4.32 Microstructures of AlZn3* sheets immersed in sea water for (a) 6 days (b) 54 days and (c) 90 days
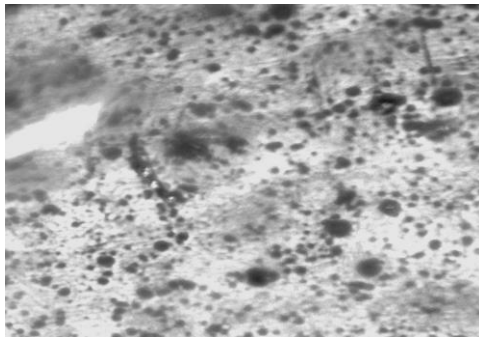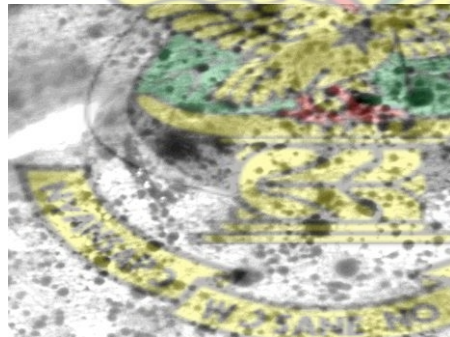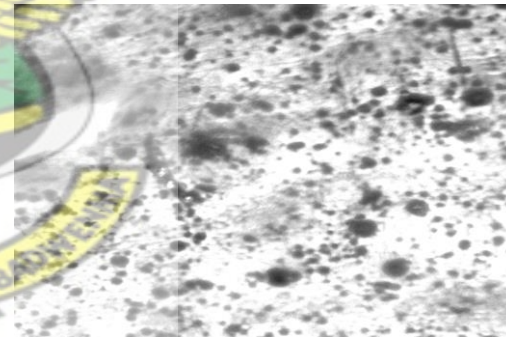
(a)   (b)   (c)

Fig 4.33 Microstructures of G1*Ind sheets immersed in sea water for (a) 6 days (b) 54 days and (c) 90 days
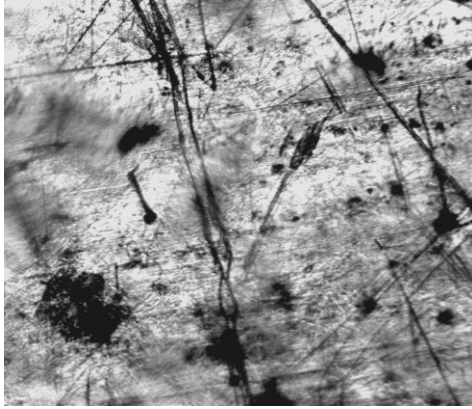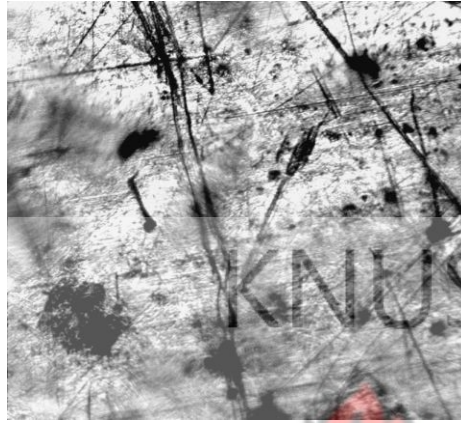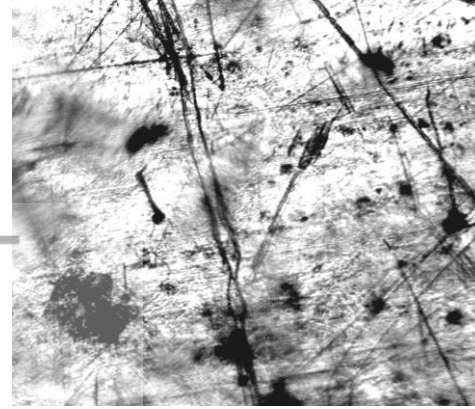
(a)   (b)   (c)
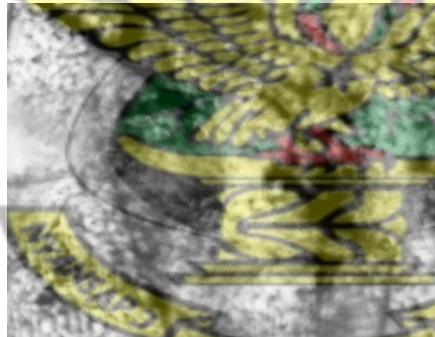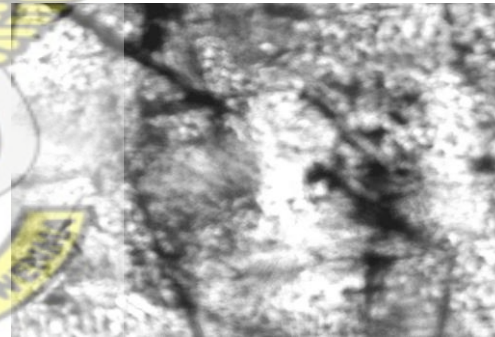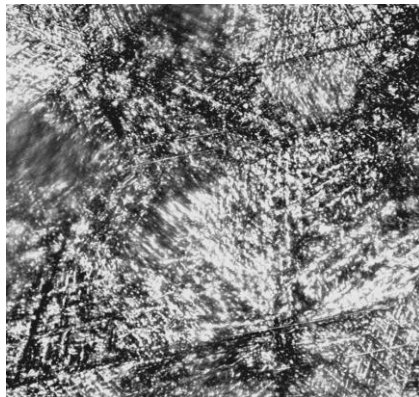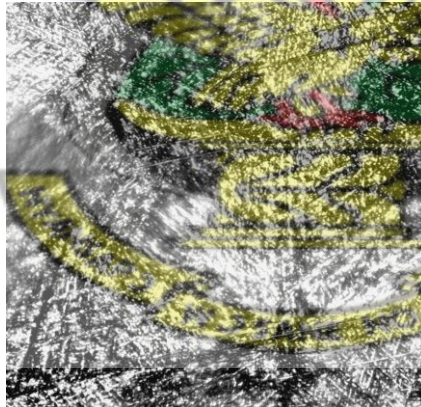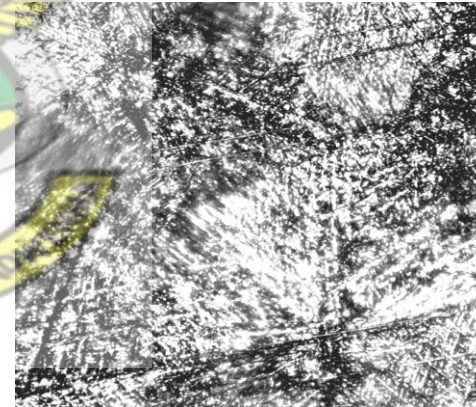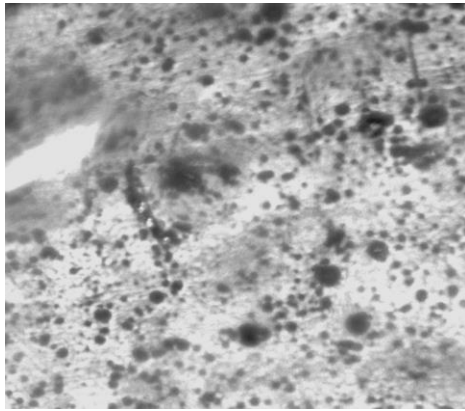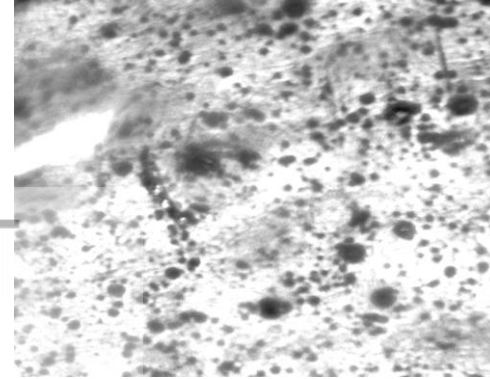
Fig 4.34 Microstructures of Al sheets immersed in sea water for (a) 6 days (b) 54 days and (c) 90 days
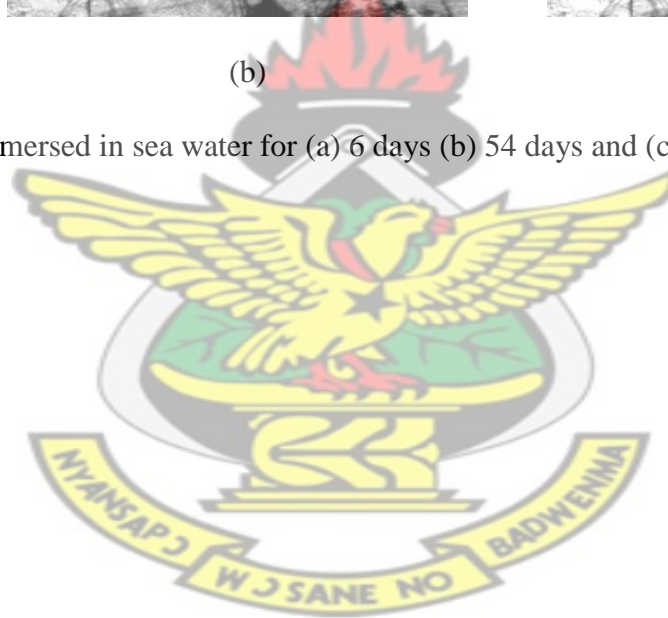
CHAPTER FIVE

CONCLUSIONS AND RECOMMENDATIONS

5.1 Conclusions

The following conclusions were drawn from the research on tensile strength, micro hardness and corrosion studies on some of the roofing sheets used in Ghana:

1. Aluzinc three star galvanized [AlZn3*] roofing sheets were observed to be very hard and brittle. This hardness property of the sheet made it possible to withstand more load, but fractured quickly just after the yield strength because of its brittleness. Aluzinc three star galvanized sheet had an average hardness value of 3875.4 ± 947.0 Nm^{-2} whiles aluminum [Al] had the least hardness value of 67.3 ± 12.99 Nm^{-2}.

2. Aluzinc three star galvanized [AlZn3*] roofing sheets were very stiff; this implies that they had a high resistance to deformation. This was clearly demonstrated by the high value of Young's Modulus of 18.2 ± 1.42 MPa than other roofing sheets. One star galvanized India [G1*Ind] sheet had the minimum average value of 7.57 ± 1.56 MPa.

3. Aluzinc three star galvanized [AlZn3*] sheets had the highest average Ultimate Tensile Strength of 50.27 ± 2.57 MPa amongst the other sheets with One star galvanized Japan [G1*Jap] having the least value of 26.9 ± 1.57 MPa.

4. The average Toughness (Break Energy) was highest for aluminum (Al) with a value of (7.97 ± 48769) 10^6 MJm^{-2} whiles One star galvanized Japan [G1*Jap] sheet the least value of

55378 $\pm$ 22666 MJm^{-2}. Aluminum [Al] roofing sheets could bear a lot of load before it fractured at a lower strain than other roofing sheets.

5. From the Percentage Elongation value which is the measure of Ductility and Toughness. Aluminum (Al) roofing sheets had the highest average Percentage Elongation of 28.2 $\pm$0.77% with One star galvanized India [G1*Ind] having the minimum average Percentage Elongation $(0.58 \pm 0.05\%)$.

6. The corrosion rate per day of different roofing sheets immersed in different solutions under the same exposure time (five months) increased with increasing exposure time. The results showed that in rain water, galvanized coated (GC) had the maximum corrosion rate per day while aluminum (Al) had the least value. In sea water, one star galvanized Japan had the maximum corrosion rate per day with galvanized coated having the least value.

7. In hydrochloric acid, the results showed that aluzinc alloy three star galvanized [AlZn3*] had the maximum corrosion rate whiles one star galvanized Japan [G1*Jap] had the least corrosion rate per day. Sodium hydroxide and acetic acid solutions recorded a highest corrosion per day values for Aluzinc three star galvanized [AlZn3*] sheets than other roofing sheets.

5.2 Recommendations and Future Work

1. Aluminum [Al] roofing sheets should often be used in building construction since it is less affected by rain water unlike galvanized coated (GC) which has a high corrosion rate per day in rain water. With the high ductility of aluminum, care should be taken during installation to prevent dent by workers.

2. Galvanized coated sheets should rather be used in coastal areas as it showed high corrosion resistance to chlorides in the sea.

3. Further work should be conducted on other roofing such as slates, fiber, clay to know their corrosion resistance under in all environments.
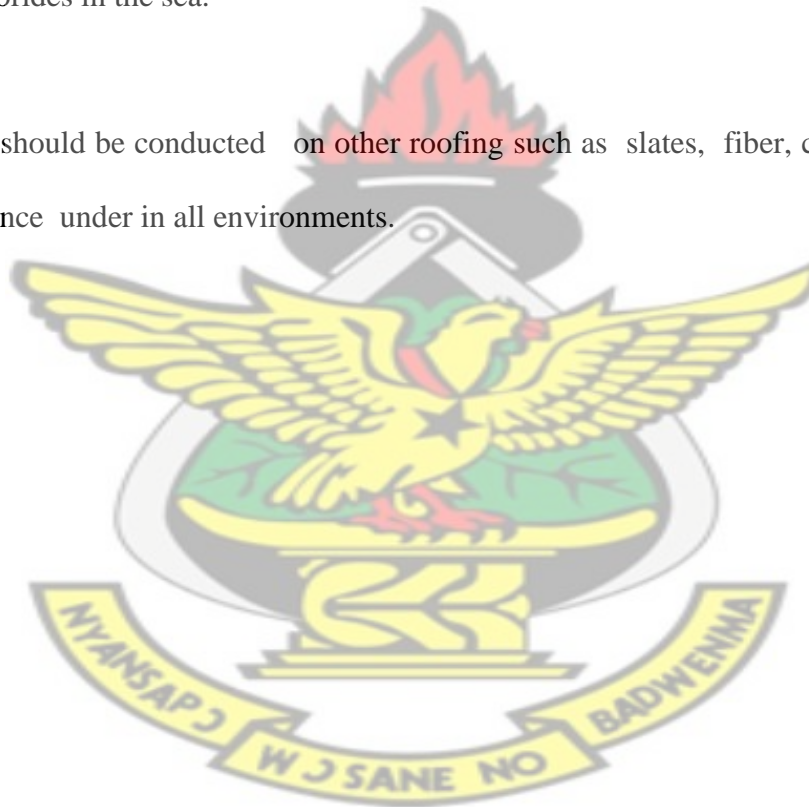
REFERENCES

N´andor G. : Roof structures in the folk architecture of the Carpathian-basin, Kolozsv´ar 1999.

V´ando A.: Roof structures, Kolozsv´ar 2000

Pomozi I.: Gothic roof structures, Kolozsv´ar 1999

Vander A. : Timbered roof structures in Hungary in the 16 - 19. century Budapest 1999.

Palladio A.: Four books of architecture on the basis of I UATTRO LIBRI DELL' ARCHITETTURA in Venezia 1570 Budapest 2006

Szab´o B.: Renovation of historic roof structures, Utilitas publication/ Kolozsv´ar 1999.

Schapcot C.: Investigation of English roof structure types, Kolozsv´ar 1999.

Makay D.: Attic-type roof structure of the Bethlen boy-college in Nagyegyed, Kolozsv´ar 1999.

Szabo B.: Introduction into the renovation- theory of historic frameworks. Kolozsv´ar 1998.

Horvath A and Abraham A. P.: Wooden roof structures in the 19th century, Budapest 2002.

Anderson D. B. and R. W. Ross Jr., "Protection of steel piling in marine splash and spray zone- Metallic sheathing concept", Proceeding 4th international congress on marine corrosion and fouling, France, pp. 461-473, 1999.

Larrablee C.P.: Corrosion resistant experimental steels for marine application, page 501-504, 2002.

Humbles A. A. "The cathodic protection of steel in seawater", Corrosion, 1999.

Boyd W.K and Fink F.W., "Corrosion of metals in marine environments", Metal & ceramic information center report, MCIC-78-37, March 2001.

Reinhart F.M. and Jenkins J.F., "Corrosion of materials in surface seawater after 12 and 18 months of exposure", Final report, NCEL-TN-1213 AD743872, January 1999.

Oldfield J.W. and Todd B, "Corrosion consideration in selected metals for flash chamber", Desalination, no. 32, (1-3), 365, 2002.

Malik A.U., Siddiq N. A., Ahmed S and Andijani I,N, Corrosion science, 37 (10), 1521-1535, 1999.

Larrabee C.P., "Corrosion resistance of high strength low alloy steel as influenced by composition and environment", Corrosion, 9, 259-371, 1999.

Hack H. P., "Corrosion behavior of 45 Mo-containing stainless steels in seawater", Corrosion 82, paper no. 65, March, 1999.

http://www.bikepro.com/products/metals/hardness.html [accessed 2010, November 24]

http://www.wargamer.org/GvA/background/hardness1.html [accessed 2010, November 24]

http://www.britannica.com/bcom/eb/article/2/0,5716,212+1,00.html

[accessed 2010, November 24]

http://www.bikepro.com/products/metals/hardness.html[accessed 2010, November 24]

LaQue F. L., "Marine corrosion and prevention", p. 116, John Wiley &sons, 1979.

Boyd W. K. and Fink F. W, "Corrosion of metals in marine environments", Metal & ceramic information center report, MCIC-78-37, March 2008.

Hart E. W.: A micromechanical basis for constitutive equations with internal state variables, Journal of Engineering Materials and Technology Transactions of the ASME, 106, 322-325, 2004.

Vuoristo T. and Kuokkala V.T.: The effect of pre-strain and loading rate on the apparent Young's modulus of dual phase steels, 2009.

Geoffrey J. L., Cambien I., and Mareuse D.: Assessment of intrinsic elastic constants by mean of both tensile test and resonance frequency measurements. In: IDDRG Working group meeting WG3/6/93, Austria 2005

Cleveland R. M. and Ghosh A. K.: Inelastic effects on springback in metals. International Journal of Plasticity, 2000

Luo L., and Ghosh A. K.: Elastic and inelastic recovery after plastic deformation of DQSK steel sheet. Journal of Engineering Materials and Technology Transactions of the ASME, 125, 3, 237-246, 2003.

APPENDICES

APPENDIX A

Error calculations

 It was calculated using the inbuilt formula in Microsoft Excel. The data for the error calculation were imported into excel and the error values were calculated by excel. The inbuilt formula use the following procedures root mean square deviation of its values from the mean: If one sample e.g. (G1*Jap) takes on N values which are real numbers then its standard deviation σ can be calculated as follows:

1. Find the mean, of the values.
2. For each value from the mean. x_i calculate its deviation (σ)
3. Calculate the squares of these deviations.
4. Find the mean of the squared deviations which is the variance σ^2.
5. Take the square root of the variance.
This calculation is described by the following formula:

$$\sigma = \sqrt{\frac{1}{N}\sum_{i=1}^{N}(x_i - \overline{x})^2},$$

Where $\overline{x}$ is the arithmetic mean.

Calculating the error values for G1*Jap

1. Young's Modulus for G1*Jap

Arithmetic Mean $(\bar{x})$ = 13.047

x_i	$(x_i - \bar{x})$	$(x_i - \bar{x})^2$
12.29	-0.76	0.5776
6.83	-6.22	38.6884
8.18	-4.87	23.7169
13.01	-0.04	0.0016
14.31	1.26	1.5876
14.19	1.14	1.2996
16.2	3.15	9.9225
12.46	-0.59	0.3481
10.3	-2.75	7.5625
22.7	9.65	93.1225

$\Sigma(x_i - \bar{x})^2 = 176.827$

Standard deviation $= \sqrt{\left(\frac{1}{10}\right)(176.627)}$

$$= \sqrt{17.6627} = 4.20$$

Error $= \dfrac{4.20}{\sqrt{10}} = 1.33$ MPa

2. Ultimate Tensile Strength for G1*Jap

Arithmetic Mean $(\bar{x})$ = 26.59

x_i	$x_i - \bar{x}$	$(x_i - \bar{x})^2$
21.6	-4.99	24.9001
38.2	11.61	134.792
30.9	4.31	18.5761
21.9	-4.69	21.9961
27.8	1.21	1.4641
27.6	1.01	1.0201
28.6	2.01	4.0401
24.8	-1.79	3.2041
21.8	-4.79	22.9441
22.7	-3.89	15.1321

$$\Sigma(x_i - \bar{x})^2 = 248.0724$$

Standard deviation $= \sqrt{\left(\frac{1}{10}\right)(248.07)}$

$$= \sqrt{24.807} = 4.981$$

Error $= \dfrac{4.981}{\sqrt{10}}$

$$= 1.57 \text{ MPa}$$

3. Percentage Elongation for G1 *Jap

Arithmetic Mean$(\bar{x})$ = 3.36

x_i	$x_i - \bar{x}$	$(x_i - \bar{x})^2$
0.26	-3.1	9.61
0.97	-2.39	5.7121
30.7	27.34	747.4756
0.278	-3.082	9.498724
0.239	-3.121	9.740641
0.1982	-3.1618	9.99697924
0.255	-3.105	9.641025
0.247	-3.113	9.690769
0.226	-3.134	9.821956
0.1845	-3.1755	10.08380025
		$\Sigma(x_i - \bar{x})^2 = 3.36$

Standard deviation = $\sqrt{\left(\frac{1}{10}\right)(3.36)}$

$= \sqrt{0.336} = 0.58$

Error = $\dfrac{0.58.}{\sqrt{10}}$

$= 0.18$ %

4. Toughness for G1*Jap

Arithmetic Mean$(\bar{x})$ = 55378

x	$x_i - \bar{x}$	$(x_i - \bar{x})2$
27000	-28378	805310884
265000	209622	43941382884
71600	16222	263153284
37900	-17478	305480484
29500	-25878	669670884
18760	-36618	1340877924
40000	-15378	236482884
32600	-22778	518837284
24000	-31378	984578884
7420	-47958	2299969764

$\Sigma(x_i - \bar{x})^2$ = 51365745160

Standard deviation = $\sqrt{\left(\frac{1}{10}\right)(51365745160)}$

$\qquad = \sqrt{5136574516} = 71669.90$

$\qquad$ Error $= \dfrac{71669.90}{\sqrt{10}}$

$\qquad\qquad = 22666.0 \text{ MJm}^{-2}$

5. Young's Modulus for GC

Arithmetic Mean $(\bar{x})$ = 11.17

x	$x_i - \bar{x}$	$(x_i - \bar{x})^2$
13.12	1.36	1.8496
11.66	-0.1	0.01
14.34	2.58	6.6564
11.29	-0.47	0.2209
8.16	-3.6	12.96
33	21.24	451.138
3.26	-8.5	72.25
1.684	-10.076	101.526
6.58	-5.18	26.8324
14.52	2.76	7.6176

$$\sum (x_i - \bar{x})^2 = 681.06$$

Standard deviation $= \sqrt{\left(\frac{1}{10}\right)(681.06)}$

$= \sqrt{68.106} = 8.25$

Error $= \dfrac{8.25}{\sqrt{10}}$

$= 2.61$ MPa

6. Toughness for GC

Arithmetic Mean $(\bar{x})$ = 177770

x	$x_i - \bar{x}$	$(x_i - \bar{x})2$
177770	253230	64125432900
177770	171230	29319712900
177770	-33770	1140412900
177770	-61070	3729544900
177770	-62970	3965220900
177770	152230	23173972900
177770	-146370	21424176900
177770	-123170	15170848900
177770	-34570	1195084900
177770	-114770	13172152900

$$\Sigma(x_i - \bar{x})^2 = 1.764 \times 10^{11}$$

Standard deviation = $\sqrt{\left(\frac{1}{10}\right)(1.76 \times 10^{11})}$
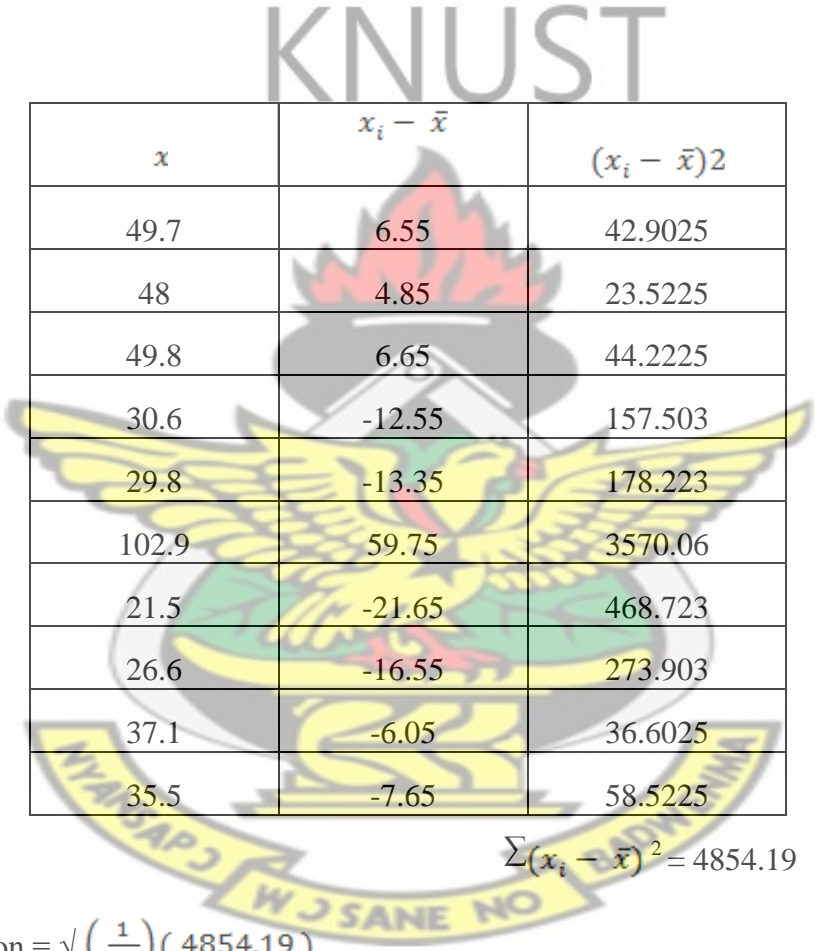
$$= \sqrt{1.76 \times 10^{10}}) = 132664$$

$$\text{Error} = \frac{132664}{\sqrt{10}}$$

$$= 41956.3 \text{ MJm}^{-2}$$

7. Ultimate Tensile Strength error for GC

Arithmetic Mean $(\bar{x}) = 43.15$

x	$x_i - \bar{x}$	$(x_i - \bar{x})2$
49.7	6.55	42.9025
48	4.85	23.5225
49.8	6.65	44.2225
30.6	-12.55	157.503
29.8	-13.35	178.223
102.9	59.75	3570.06
21.5	-21.65	468.723
26.6	-16.55	273.903
37.1	-6.05	36.6025
35.5	-7.65	58.5225

$$\Sigma(x_i - \bar{x})^2 = 4854.19$$

$$\text{Standard deviation} = \sqrt{\left(\frac{1}{10}\right)(4854.19)}$$

$$= \sqrt{1485.419} = 22.03$$

$$\text{Error} = \frac{22.03}{\sqrt{10}}$$

$$= 6.97 \text{ MPa}$$

8. Percentage Elongation error for GC

Arithmetic Mean $(\bar{x})$ = 5.05

x	$x_i - \bar{x}$	$(x_i - \bar{x})2$
1.194	-3.856	14.868736
0.993	-4.057	16.459249
0.472	-4.578	20.958084
0.539	-4.511	20.349121
0.575	-4.475	20.025625
44.5	39.45	1556.3025
0.456	-4.594	21.104836
0.734	-4.316	18.627856
0.682	-4.368	19.079424
0.353	-4.697	22.061809

$$\Sigma (x_i - \bar{x})^2 = 1729.84$$

Standard deviation = $\sqrt{\left(\frac{1}{10}\right)(1729.84)}$

$$= \sqrt{172.984} = 13.15$$

$$\text{Error} = \frac{13.15}{\sqrt{10}}$$

$$= 4.16\%$$

9. Young's Modulus error for AlZn3*

Arithmetic Mean $(\bar{x}) = 18.2$

x	$x_i - \bar{x}$	$(x_i - \bar{x})2$
27.8	9.6	92.16
22.4	4.2	17.64
17.04	-1.16	1.3456
17.04	-1.16	1.3456
17.8	-0.4	0.16
17.8	-0.4	0.16
9.66	-8.54	72.9316
20.5	2.3	5.29
16.53	-1.67	2.7889
15.47	-2.73	7.4529

$$\Sigma(x_i - \bar{x})^2 = 201.275$$

$$\text{Standard deviation} = \sqrt{\left(\frac{1}{10}\right)(201.275)}$$

$$= \sqrt{20.1275} = 4.49$$

$$\text{Error} = \frac{4.49}{\sqrt{10}}$$

= 1.42 MPa

10. Toughness error for AlZn3*

Arithmetic Mean($\bar{x}$) = 316810

x	$x_i - \bar{x}$	$(x_i - \bar{x})^2$
30600	-286210	81916164100
29500	-287310	82547036100
642000	325190	1.05749E+11
642000	325190	1.05749E+11
84000	-232810	54200496100
84000	-232810	54200496100
335000	18190	330876100
320000	3190	10176100
456000	139190	19373856100
545000	228190	52070676100

$\Sigma(x_i - \bar{x})^2 = 5.561 \times 10^{11}$

Standard deviation $= \sqrt{\left(\frac{1}{10}\right)(5.561 \times 10^{11})} = \sqrt{5.561 \times 10^{10}} = 235817.7$

$$\text{Error} = \frac{4235817.7}{\sqrt{10}}$$

$$= 74578.7 \text{ MJm}^{-2}$$

11. Ultimate Tensile Strength error for AlZn3*

Arithmetic Mean $(\bar{x})$

$= 50.27$

x	$x_i - \bar{x}$	$(x_i - \bar{x})2$
45.2	-5.07	25.7049
30.7	-19.57	382.985
60.3	10.03	100.601
60.3	10.03	100.601
47.6	-2.67	7.1289
47.6	-2.67	7.1289
49.5	-0.77	0.5929
53.3	3.03	9.1809
54.5	4.23	17.8929
53.7	3.43	11.7649

$$\Sigma(x_i - \bar{x})^2 = 663.58$$

Standard deviation = $\sqrt{\left(\frac{1}{10}\right)(663.58)}$

$= \sqrt{66.358} = 8.14$

Error = $\dfrac{8.14}{\sqrt{10}}$

$= 2.57 \text{ MPa}$

KNUST

12. Percentage Elongation error for AlZn3*

Arithmetic Mean $(\bar{x}) = 0.88$

x	$x_i - \bar{x}$	$(x_i - \bar{x})2$
0.837	-0.043	0.001849
0.1728	-0.7072	0.50013184
1.624	0.744	0.553536
1.624	0.744	0.553536
0.315	-0.565	0.319225
0.315	-0.565	0.319225
0.955	0.075	0.005625
0.751	-0.129	0.016641
1.033	0.153	0.023409
1.208	0.328	0.107584

$$\Sigma(x_i - \bar{x})^2 = 2.4$$

Standard deviation = $\sqrt{\left(\frac{1}{10}\right)(2.4)}$

$= \sqrt{0.24} = 0.49$

Error = $\dfrac{0.49}{\sqrt{10}}$

$= 0.15\%$

13. Young's Modulus for G1*Ind

Arithmetic Mean $(\bar{x}) = 7.57$

x_i	$x_i - \bar{x}$	$(x_i - \bar{x})2$
14.52	6.95	48.3025
2.2	-5.37	28.8369
14.2	6.63	43.9569
8.53	0.96	0.9216
5.43	-2.14	4.5796
3.35	-4.22	17.8084
1.684	-5.886	34.645
3.26	-4.31	18.5761
8.16	0.59	0.3481
14.34	6.77	45.8329

$$\Sigma(x_i - \bar{x})^2 = 243.80$$

Standard deviation = $\sqrt{\left(\frac{1}{10}\right)(243.80)}$

$\qquad = \sqrt{24.380} = 4.93$

Error = $\dfrac{4.93}{\sqrt{10}}$

$\qquad = 1.56$ MPa

14. Ultimate Tensile Strength for G1*Ind

Arithmetic Mean$(\bar{x}) = 32.31$

x	$x_i - \bar{x}$	$(x_i - \bar{x})2$
35.5	3.19	10.1761
32.2	-0.11	0.0121
27.9	-4.41	19.4481
37.1	4.79	22.9441
39.1	6.79	46.1041
23.6	-8.71	75.8641
26.6	-5.71	32.6041
21.5	-10.81	116.856
29.8	-2.51	6.3001
49.8	17.49	305.9

$\Sigma(x_i - \bar{x})^2 = 636.21$

Standard deviation $= \sqrt{\left(\frac{1}{10}\right)(636.21)}$

$= \sqrt{63.621} = 7.98$

Error $= \dfrac{7.98}{\sqrt{10}}$

$= 2.52$ MPa

15. Toughness for G1*Ind

Arithmetic Mean$(\bar{x})$ = 92230

x	$x_i - \bar{x}$	$(x_i - \bar{x})^2$
63000	-29230	854392900
94600	2370	5616900
52700	-39530	1562620900
143200	50970	2597940900
168100	75870	5756256900
55900	-36330	1319868900
54600	-37630	1416016900
31400	-60830	3700288900
114800	22570	509404900
144000	51770	2680132900

$$\Sigma(x_i - \bar{x})^2 = 20403541000$$

Standard deviation = $\sqrt{\left(\frac{1}{10}\right)(20402541000)}$

$= \sqrt{2040254100} = 45169.17$

Error $= \dfrac{45169.17}{\sqrt{10}}$

$= 14285.0 \text{ MJ/m}^2$

16. Percentage Elongation for G1*Ind

Arithmetic Mean$(\bar{x}) = 0.58$

x	$x_i - \bar{x}$	$(x_i - \bar{x})^2$
0.353	-0.227	0.051529
0.847	0.267	0.071289
0.33	-0.25	0.0625
0.682	0.102	0.010404
0.776	0.196	0.038416
0.559	-0.021	0.000441
0.734	0.154	0.023716
0.456	-0.124	0.015376
0.575	-0.005	0.000025
0.472	-0.108	0.011664

$$\sum(x_i - \bar{x})^2 = 0.28536$$

Standard deviation $= \sqrt{\left(\frac{1}{10}\right)(0.28536)}$

$= \sqrt{0.028536} = 0.1689$

Error $= \dfrac{0.17}{\sqrt{10}}$

$= 0.05\%$

17 Young's Modulus error for Al

Arithmetic Mean $(\bar{x})$ = 17.99

x	$x_i - \bar{x}$	$(x_i - \bar{x})^2$
44.5	26.51	702.78
0.602	-17.388	302.343
0.1085	-17.882	319.748
7.21	-10.78	116.208
17.44	-0.55	0.3025
20.3	2.31	5.3361
44.5	26.51	702.78
0.602	-17.388	302.343
0.1085	-17.882	319.748
44.5	26.51	702.78

$$\Sigma(x_i - \bar{x})^2 = 3474.37$$

Standard deviation $= \sqrt{\left(\frac{1}{10}\right)(3474.37)}$

$$= \sqrt{347.4} = 18.64$$

$$\text{Error} = \frac{18.64}{\sqrt{10}}$$

$$= 5.89 \text{ MPa}$$

18. Ultimate Tensile Strength for Al

Arithmetic Mean$(\bar{x})$ = 37.52

x	$x_i - \bar{x}$	$(x_i - \bar{x})^2$
48.2	10.68	114.062
27.9	-9.62	92.5444
17.4	-20.12	404.814
47.9	10.38	107.744
46.6	9.08	82.4464
45.5	7.98	63.6804
48.2	10.68	114.062
27.9	-9.62	92.5444
17.4	-20.12	404.814
48.2	10.68	114.062

$$\Sigma(x_i - \bar{x})^2 = 1590$$

Standard deviation $= \sqrt{\left(\frac{1}{10}\right)(1590.78)}$

$= \sqrt{159.078} = 12.61$

Error $= \dfrac{12.61}{\sqrt{10}}$

$= 3.99$ MPa

19. Percentage Elongation for Al

Arithmetic mean = 28.2

x	$x_i - \bar{x}$	$(x_i - \bar{x})^2$
28.5	0.3	0.09
27.8	-0.4	0.16
32.2	4	16
27.1	-1.1	1.21
24.2	-4	16
25.2	-3	9
28.5	0.3	0.09
27.8	-0.4	0.16
32.2	4	16
28.5	0.3	0.09

$$\Sigma(x_i - \bar{x})^2 = 58.8$$

Standard deviation $= \sqrt{\left(\frac{1}{10}\right)(58.8)}$

$\qquad = \sqrt{5.88} = 2.42$

Error $= \dfrac{2.42}{\sqrt{10}}$

$\qquad = 0.77\%$

20. Toughness for Al

Arithmetic mean = 7956600

x	$x_i - \bar{x}$	$(x_i - \bar{x})^2$
12750000	4793400	2.29767E+13
658000	-7298600	5.32696E+13
3730000	-4226600	1.78641E+13
11860000	3903400	1.52365E+13
10260000	2303400	5.30565E+12
10420000	2463400	6.06834E+12
12750000	4793400	2.29767E+13
658000	-7298600	5.32696E+13
3730000	-4226600	1.78641E+13
12750000	4793400	2.29767E+13

$$\sum(x_i - \bar{x})^2 = 2.378 \times 10^{14}$$

Standard deviation $= \sqrt{\left(\frac{1}{10}\right)(2.378 \times 10^{14})}$

$$= \sqrt{2.378 \times 10^{13}} = 4876556$$

Error $= \dfrac{4876556}{\sqrt{10}}$

$$= 1542237.8 \text{ MJ/m}^2$$

Table 1 Average Tensile Tests of Modulus of Elasticity, Ultimate Tensile Strength, Percentage Elongation and Toughness for various samples

Sample Identity	Modulus of Elasticity (Mpa)	Ultimate Tensile Strength (Mpa)	Percentage Elongation (%)	Toughness (MJm^{-2})
G1*Jap	13.047	26.59	3.35577	55378
GC	11.7614	43.15	5.0498	177770
AlZn3*	18.204	50.27	0.88348	316810
G1*Ind	7.5674	32.31	0.5784	92230
Al	17.9871	37.52	28.2	79366600

APPENDIX B

TENSILE TEST GRAPGHS FROM TINIUS OLSEN SUPER 'L'
HYDRAULIC TESTING MACHINE UNIVERSAL
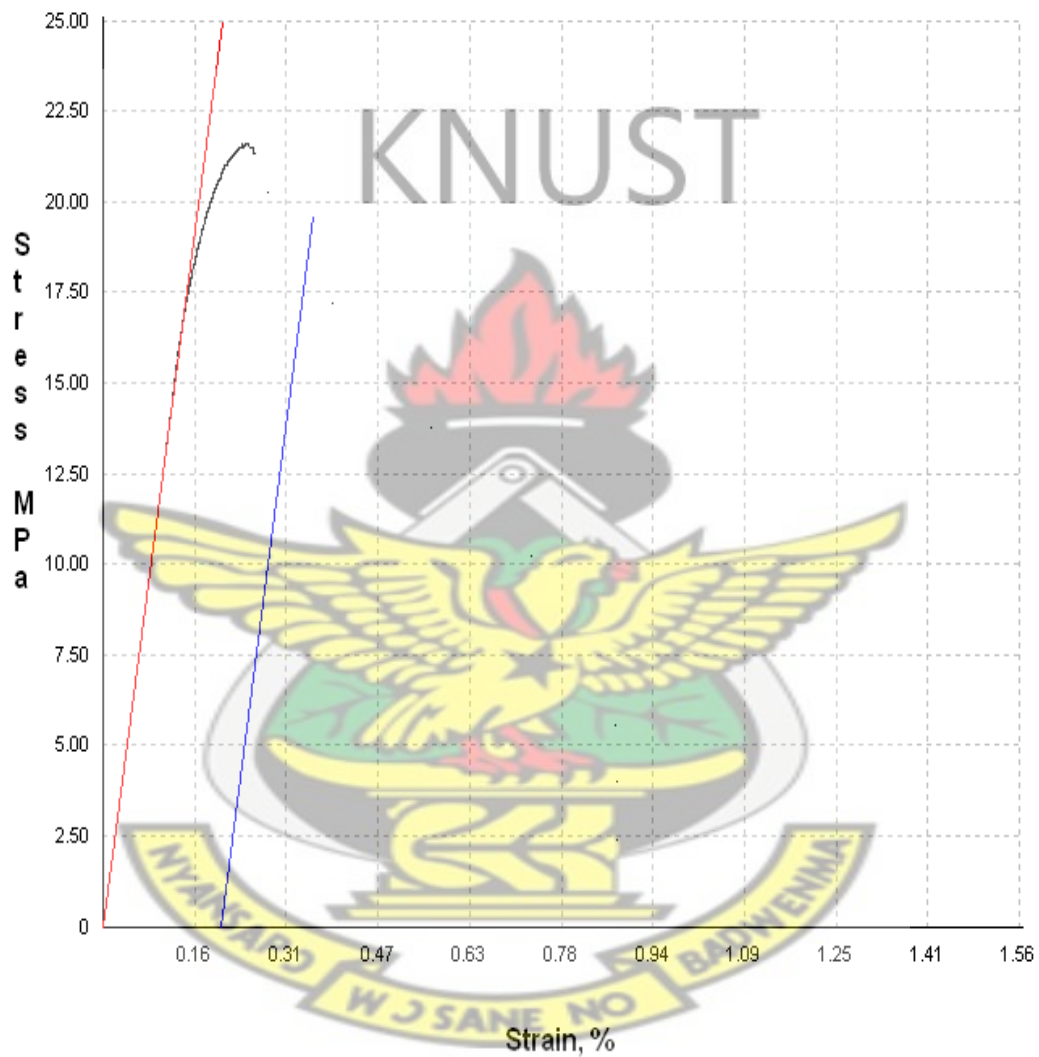
Fig, 1 Tensile Test graph for One star galvanized Japan
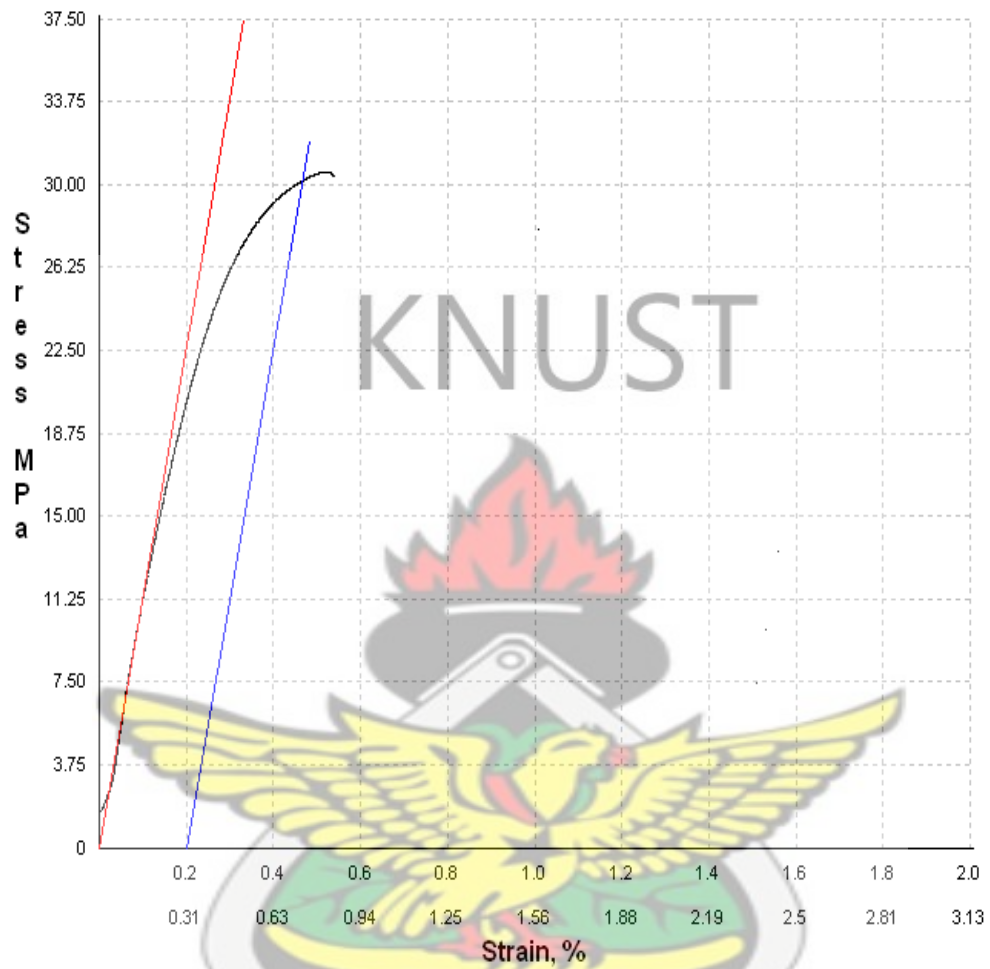
Fig, 2 Tensile Test graph for Galvanized coated roofing sheets
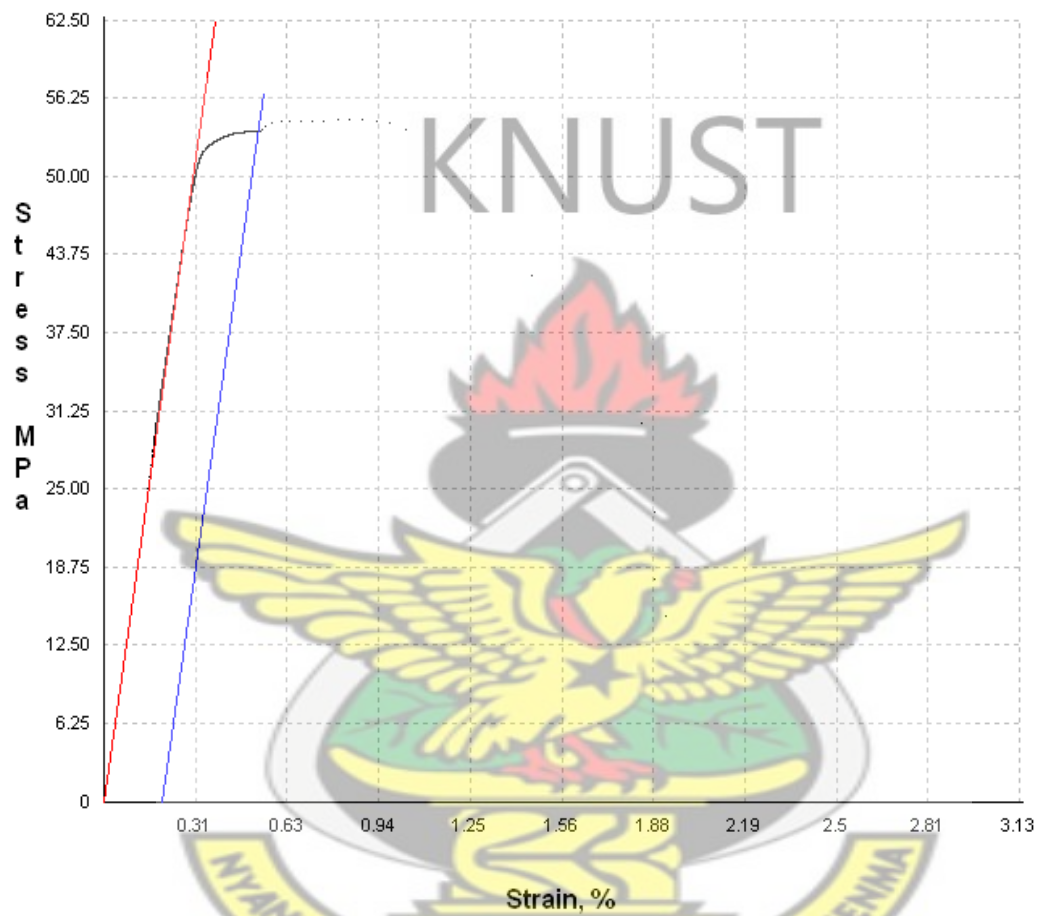
Fig, 3 Tensile Test graph for Aluzinc three star galvanized
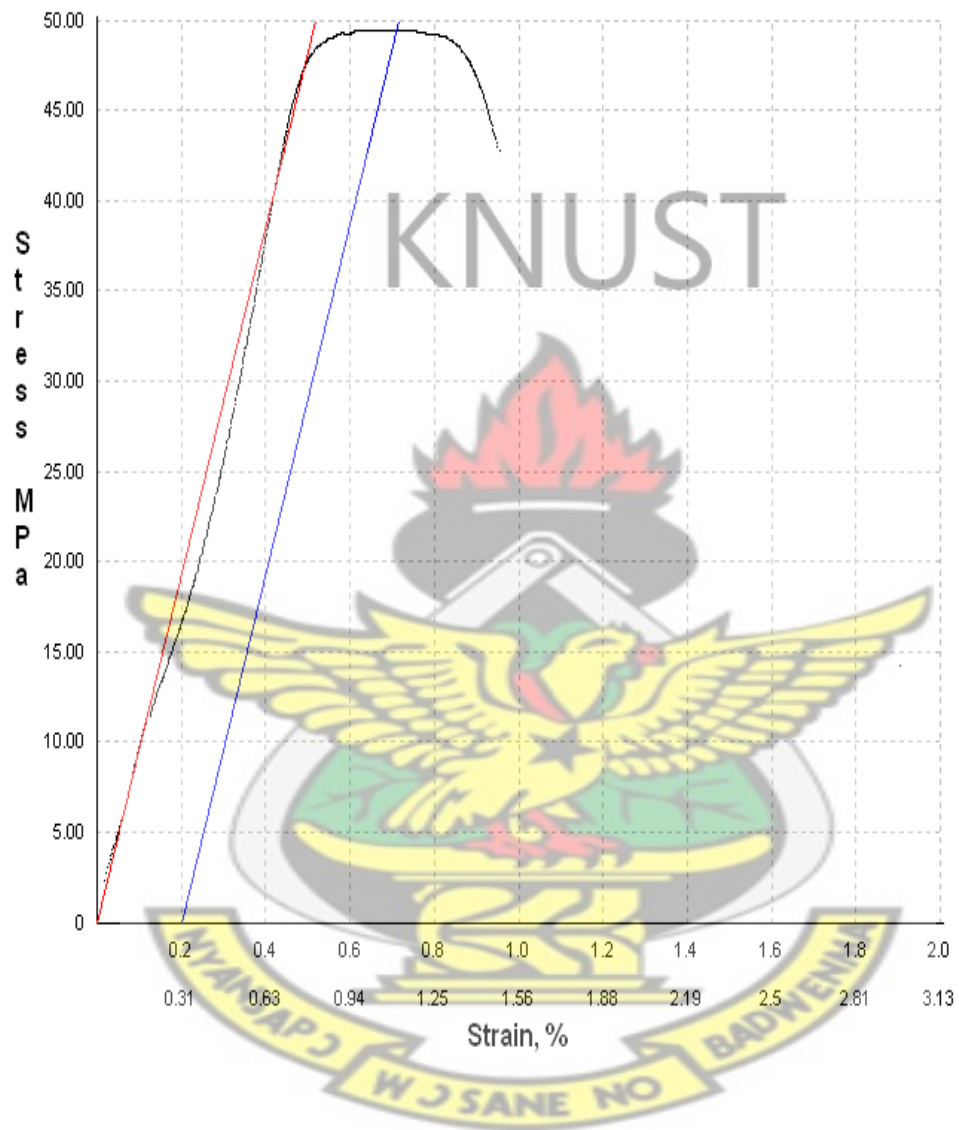
Fig, 4 Tensile Test graph for One star galvanized India
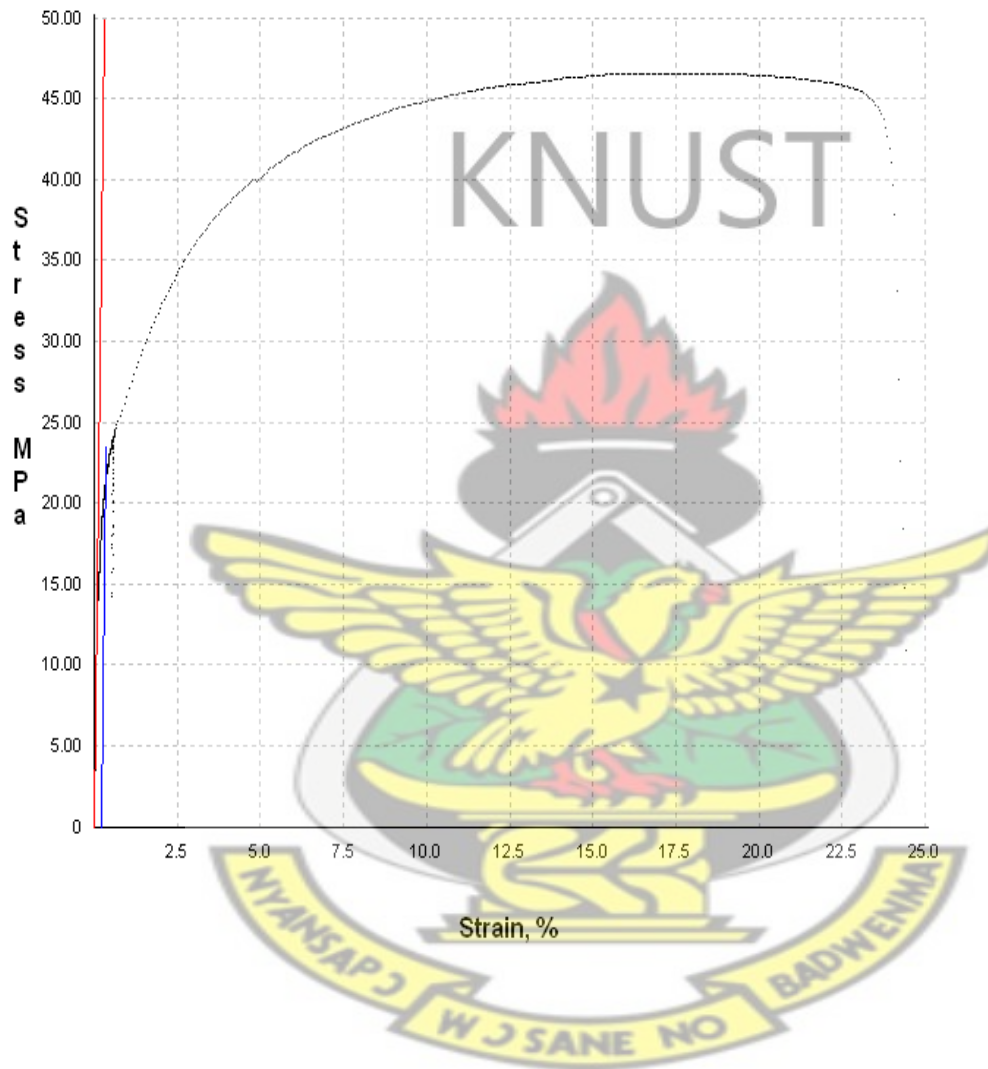
Fig. 5 Tensile Test graph for Aluminium sheets

APPENDIX C

Table 2 Micro Hardness of One star galvanized sheets

Nr	d1(mm)	d2(mm)	HV
1	0.1404	0.1404	751.3
2	0.1459	0.1459	936.7
3	0.1544	0.1544	777.6
4	0.1599	0.1599	725.2
5	0.1997	0.1997	444.2
6	0.2133	0.2133	407.5
7	0.2183	0.2183	389.1
8	0.2216	0.2216	377.6
9	0.2312	0.2312	323.8
10	0.2321	0.2321	352
11	0.2353	0.2353	334.9
12	0.2375	0.2375	288.7
13	0.2436	0.2436	277
14	0.2604	0.2604	292.4
15	0.2716	0.2716	251.3
16	0.2729	0.2729	253.2
17	0.274	0.274	264.9
18	0.2747	0.2747	245.7
19	0.2793	0.2793	237.7
20	0.2795	0.2795	237.3
21	0.2806	0.2806	235.5
22	0.2879	0.2879	223.7
23	0.2913	0.2913	218.5
24	0.325	0.325	175.5
25	0.3479	0.3479	158.1

Table 3 Micro Hardness of Galvanized coated sheets

Nr	d1(mm)	d2(mm)	HV
1	0.1404	0.1404	751.3
2	0.1459	0.1459	936.7
3	0.1544	0.1544	777.6
4	0.1599	0.1599	725.2
5	0.1997	0.1997	444.2
6	0.2133	0.2133	407.5
7	0.2183	0.2183	389.1
8	0.2216	0.2216	377.6
9	0.2312	0.2312	323.8
10	0.2321	0.2321	352
11	0.2353	0.2353	334.9
12	0.2375	0.2375	288.7
13	0.2436	0.2436	277
14	0.2604	0.2604	292.4
15	0.2716	0.2716	251.3
16	0.2729	0.2729	253.2
17	0.274	0.274	264.9
18	0.2747	0.2747	245.7
19	0.2793	0.2793	237.7
20	0.2795	0.2795	237.3
21	0.2806	0.2806	235.5
22	0.2879	0.2879	223.7
23	0.2913	0.2913	218.5
24	0.325	0.325	175.5
25	0.3479	0.3479	158.1

Table 3 Micro Hardness of Aluzinc three star galvanized sheets

Nr	d1(mm)	d2(mm)	HV
1	0.0106	0.0106	1650.3
2	0.0264	0.0264	392.1
3	0.0264	0.0264	392.1
4	0.0269	0.0269	5965.8
5	0.0276	0.0276	4683.4
6	0.0295	0.0295	1647.6
7	0.0313	0.0313	5820.9
8	0.0316	0.0316	5463.2
9	0.0317	0.0317	5346.2
10	0.0332	0.0332	3716.4
11	0.0339	0.0339	3028.8
12	0.0342	0.0342	2746.9
13	0.0345	0.0345	2472.4
14	0.0345	0.0345	2472.4
15	0.0351	0.0351	5581.3
16	0.0392	0.0392	5514
17	0.0395	0.0395	5331.4
18	0.0397	0.0397	5212
19	0.0397	0.0397	5212
20	0.04	0.04	5036.1
21	0.0428	0.0428	3569.3
22	0.0457	0.0457	2325.3
23	0.0534	0.0534	6527.4
24	0.0557	0.0557	5977
25	0.262	0.262	799.8

Table 4 Micro Hardness of One star galvanized India sheets

Nr	d1(mm)	d2(mm)	HV
1	0.2165	0.2165	429
2	0.2185	0.2185	399.6
3	0.232	0.232	366.9
4	0.2608	0.2608	267.6
5	0.2625	0.2625	269.1
6	0.2763	0.2763	242.9
7	0.2807	0.2807	255.8
8	0.2815	0.2815	264.2
9	0.2935	0.2935	199.6
10	0.3076	0.3076	199.7
11	0.3086	0.3086	200.6
12	0.3215	0.3215	179.4
13	0.3249	0.3249	182.6
14	0.3318	0.3318	194
15	0.3347	0.3347	172.8
16	0.3511	0.3511	152.1
17	0.3562	0.3562	149.7
18	0.396	0.396	128.4
19	0.4293	0.4293	111.1
20	0.4482	0.4482	95.6
21	0.4635	0.4635	108.7
22	0.4733	0.4733	100.8
23	0.4825	0.4825	97.5
24	0.5339	0.5339	67.3
25	0.6474	0.6474	52.5

Table 5 Micro Hardness of Aluminium sheets

Nr	d1(mm)	d2(mm)	HV
1	0.3669	0.3669	137.7
2	0.3669	0.3669	123.9
3	0.3868	0.3868	67.5
4	0.3979	0.3979	117.1
5	0.4676	0.4676	84.8
6	0.4783	0.4783	81
7	0.4798	0.4798	80.5
8	0.4959	0.4959	75.4
9	0.5054	0.5054	72.5
10	0.5055	0.5055	72.5
11	0.5323	0.5323	65.4
12	0.5337	0.5337	65.1
13	0.5358	0.5358	64.5
14	0.5423	0.5423	63
15	0.5661	0.5661	57.8
16	0.5713	0.5713	56.8
17	0.5884	0.5884	53.5
18	0.5906	0.5906	53.1
19	0.6207	0.6207	48.1
20	0.6245	0.6245	47.5
21	0.66	0.66	42.5
22	0.6757	0.6757	40.6
23	0.68	0.68	40.1
24	0.7077	0.7077	37
25	0.7303	0.7303	34.7

APPENDIX D

Table 6 Corrosion rate per day for each sample immersed in different solutions for 6 days

Solution	G1*Jap	GC	AlZn3*	G1*Ind	AL
Rain water	0.0001633	0.0001466	0.0001567	0.0001767	0.000111
Sea water	0.0001933	0.0001333	0.0001243	0.0001467	0.0001164
HCl	0.001133	0.001877	0.001633	0.001333	0.001484
NaOH	0.001167	0.001116	0.001476	0.001167	0.001237
Acetic acid	0.001047	0.001012	0.001224	0.001067	0.001345

Table 7 Corrosion rate per day for each sample immersed in different solutions for
16 days

Solution	G1*Jap	GC	AlZn3*	G1*Ind	AL
Rain water	0.0001633	0.000147	0.0001567	0.0001767	0.000111
Sea water	0.0001933	0.000133	0.0001243	0.0001467	0.0001164
HCl	0.002133	0.003877	0.002633	0.004333	0.002484
NaOH	0.002167	0.002116	0.003476	0.004167	0.003237
Acetic acid	0.001047	0.001012	0.001224	0.001067	0.001345

Table 8 Corrosion rate per day for each sample immersed in different solutions for 25 days

Solution	G1*Jap	GC	AlZn3*	G1*Ind	AL
Rain water	0.0001633	0.000147	0.0001567	0.0001767	0.000111
Sea water	0.0001933	0.000133	0.0001243	0.0001467	0.0001164
HCl	0.001133	0.001877	0.001633	0.001333	0.001484
NaOH	0.001167	0.001116	0.001476	0.001167	0.001237
Acetic acid	0.001047	0.001012	0.001224	0.001067	0.001345

Table 9 Corrosion rate per day for each sample immersed in different solutions for 54 days

Solution	G1*Jap	GC	AlZn3*	G1*Ind	AL
Rain water	0.0003556	0.000463	0.0002567	0.0003704	0.0002255
Sea water	0.0004358	0.000769	0.0004122	0.0008425	0.0002704
HCl	0.001477	0.002191	0.00225	0.001857	0.001954
NaOH	0.001325	0.001345	0.002036	0.001469	0.001375
Acetic acid	0.001178	0.001192	0.001622	0.001223	0.001594

Table 10 Corrosion rate per day for each sample immersed in different solutions for 75 days

Rain water	0.0003556	0.000463	0.0002567	0.0003704	0.0002255
Sea water	0.0004358	0.000769	0.0004122	0.0008425	0.0002704
HCl	0.001476	0.00219	0.002248	0.001855	0.001954
NaOH	0.001325	0.001346	0.002037	0.0014109	0.001376
Acetic acid	0.001178	0.001193	0.001623	0.001224	0.001595

Table 11 Corrosion rate per day for each sample immersed in different solutions for 90 days

Solution	G1*Jap	GC	AlZn3*	G1*Ind	AL
Rain water	0.0006704	0.000976	0.000433	0.000578	0.0002975
Sea water	0.0009841	0.000529	0.0004556	0.0009431	0.0003422
HCl	0.001786	0.002422	0.0028125	0.0023811	0.002375
NaOH	0.001732	0.00154	0.002619	0.002135	0.002054
Acetic acid	0.0014692	0.001271	0.002111	0.001403	0.001632

Table 12 Corrosion rate per day for each sample immersed in different solutions for 101 days

Solution	G1*Jap	GC	AlZn3*	G1*Ind	AL
Rain water	0.0006704	0.000976	0.000433	0.000578	0.0002975
Sea water	0.0009841	0.000529	0.0004556	0.0009431	0.0003422
HCl	0.001787	0.002459	0.0028127	0.002393	0.002377
NaOH	0.001737	0.001594	0.002615	0.002139	0.002057
Acetic acid	0.001499	0.001276	0.002117	0.001412	0.001637

KNUST

KNUST